(15) 46p.

UNLIMITED

(14) RAE-TR-77161

(2) (19) BR-62228.

(18) DRIC

ROYAL AIRCRAFT ESTABLISHMENT

*

(9) Technical Report

(11) November 1977

(6)

THE MIRANDA (X4) INFRA-RED EXPERIMENT: DESIGN, PERFORMANCE AND EARTH RADIANCE MEASUREMENTS.

by

(10) M.B. Barnes,
S. Craig
A. Haskell

78 09 05* 145

Procurement Executive, Ministry of Defence

Farnborough, Hants

UNLIMITED

310 450

ROYAL AIRCRAFT ESTABLISHMENT

THE MIRANDA (X4) INFRA-RED EXPERIMENT: DESIGN,
PERFORMANCE AND EARTH RADIANCE MEASUREMENTS

by

M. B. Barnes

S. Craig

A. Haskell

SUMMARY

A description of the infra-red experiment carried on the UK Miranda (X4) satellite is given. The performance of the four pyro-electric detectors used in the experiment is described and details of the technique used for measuring the radiance of the earth in the band 14-16 μm are presented. Finally the measured radiance of the earth is shown for periods at monthly intervals from March to November 1974 and the implications of these results for the design of infra-red earth sensors are discussed.

2

LIST OF CONTENTS

161

1   INTRODUCTION

On 9 March 1974 the UK satellite Miranda (X4), international designation 1974-13A, was launched on a scout vehicle into a nominally sun-synchronous orbit with its plane perpendicular to the sun line and with apogee and perigee at 930 km and 720 km respectively. The prime objective of the Miranda mission was to prove the satellite's inertial and sun referenced 3 axis attitude control system. This control system maintains the satellite pitch axis sunpointing.

The X4 project originally included meteorological experiments which were withdrawn after the project had been running for about a year leaving space in the satellite to include a number of attitude sensing experiments. New experiments were permitted at this stage on the understanding that only very small changes to the satellite systems were acceptable. The experiments chosen included a star sensor, an albedo sensor and an Infra-red Earth Sensor which is the subject of this report. The infra-red sensor included four pyro-electric detectors of a type then being developed by Mullard Ltd for space use. The principal objective of the infra-red experiment was to gain information about the performance of these detectors but it was also decided that the opportunity should be taken to measure the radiance of the earth in the spectral interval 14-16 μm. The sensor was also used to determine pitch attitude and to provide a warning signal to the attitude control system if the earth was in, or close to, the field of view of the star sensor, Experiment C.

2   THE DETECTOR

2.1   Detector description

The detectors were manufactured by Mullard Ltd at Southampton and designated Type P200X. They were produced under MOD Contract K70B/428 to develop a Deuterated, Aniline doped, Triglycine Sulphate (TGS) detector suitable for use in spacecraft IR sensors. The active area of the detector flake was 0.55 mm square. A conical nickel reflecting light pipe, a germanium field lens and field stop were used to produce a detector with an entrance aperture 3 mm x 1 mm and a conical polar response of semiangle 7°.

A pre-amplifier with a voltage gain of 5, constructed using thick-film hybrid techniques, was incorporated into the detector package shown in Fig 1. All measurements taken on the detector were referred to the output of this pre-amplifier. The components were mounted in a stainless steel package. After being dried thoroughly by baking in a vacuum at $+70^{\circ}$C the package was then

4

filled with dry nitrogen and sealed using an epoxy resin adhesive. Appendix A gives an outline specification for the detector.

2.2   Detector characteristics

During the development and evaluation of the P200X in the laboratory two unfortunate characteristics of the detectors became evident. These were subsequently named Thermally Induced Transients and Thermally Induced Noise.

Thermally Induced Transients are the near instantaneous release of charge in sufficient quantity to give voltage pulses at the detector output of up to several millivolts. An example of these is shown in Fig 2. They were found only when the temperature of the detector was changing and were observed with rates of change of temperature of as low as $1^{\circ}C$ per hour. It was also found that an increase in the rate of change of temperature increased the frequency of occurrence of the transients but not the amplitude.

Although this experiment was not very susceptible to the effect of these transients it was appreciated that in some applications their presence would render the detector unusable and, as a result, work at RSRE Malvern and at Mullard has been undertaken in an attempt to eliminate them from the detectors. Since the X4 satellite programme did not allow time for further development of the detectors it was necessary to use the devices currently available. All of the detectors available to us were therefore screened by monitoring the transient voltage excursions as the detectors were cycled through the required operating temperature range and the devices showing fewest transients in this temperature range were selected for flight use.

Thermally induced noise was a far more serious problem in the Miranda experiment. This phenomenon is best described as a sudden increase in noise output from the device by up to a factor of 10 after several temperature cycles of amplitude 5 to $10^{\circ}C$. It was found that this increase in noise was sometimes temporary and that the affected detector would revert to the low noise "normal" condition and continue to operate satisfactorily. It was generally true however, that detectors which became noisy would eventually change permanently to the high noise (failed) state. A complete solution to this problem could not be found within the timescale of the Miranda programme. However improvements in fabrication techniques and quality control did lead to an improvement in the situation and the gross effects of this noise were not seen in any of the flight detectors prior to launch.

Subsequent work at Mullard and at the RSRE (Malvern) in 1974-75 has shown that the noise is caused mainly by the effects of moisture on the polished surface and electrodes of the TGS element. The tendency to become noisy can be prevented by processing in dry conditions and then mounting the TGS element in a vacuum tight package filled with very dry inert gas.

The detectors were carefully tested and calibrated before incorporation into the experimental package. The responsivity and noise of each detector was measured as a function of temperature and the variation in responsivity across the entrance aperture was also measured. The broadband noise from the detectors was monitored periodically and the dc working point of the internal pre-amplifier was also checked from time to time. Finally the polar response of the detectors was checked to test the quality of the light pipe. Curves of responsivity versus temperature for the 4 detectors flown are shown in Fig 3 and a typical polar response is shown in Fig 4.

On the basis of transient and noise measurements the worst detectors were rejected*.

3 THE SENSOR

3.1 The sensor design

The IR sensor consisted of a radiometer with 4 detectors which were closely grouped to enable one oscillating segmented disc to chop the radiation from 4 separate fields of view. Fig 5 shows the major sub-assemblies of the sensor. The cylindrical package was composed of 4 basic demountable parts:

(i) Optical Head.
(ii) IR Modulator.
(iii) Detector assembly.
(iv) Electronic package.

Accurate and repeatable alignment of parts (i), (ii) and (iii) was achieved by spigot and dowel fits at each interface. The sensor, shown in Fig 6, weighed 1.4 kg and was 114 mm dia and 200 mm long.

---

* The detectors selected for use were matched into 4 pairs with similar temperature coefficients of responsivity. These pairs were allocated to provide matching of channels 1 with 2 and 3 with 4 in both the flight and flight spare sensors. After assembly into the experimental package the performance of the detectors was monitored via the calibration procedure applied to the experiment as a whole.

Each channel had a field of view of $3^{\circ} \times 1^{\circ}$. The fields of view of channels 1 and 2 were parallel and aligned in the pitch plane at an angle of 153.3° to the positive roll axis, see Fig 7. These two fields of view were arranged to have their 3° dimension perpendicular to the pitch plane. Channels 3 and 4 were also aligned in the pitch plane, but with their 1° dimension perpendicular to pitch plane and with channels 3 and 4 at angles of 164° and 20° to the positive roll axis respectively, see Fig 7. Channel 4 was oriented in a direction opposite to that of the star sensor field of view and the included angle between channels 3 and 4 was greater than the angular subtense of the earth. It could thus be deduced that whenever the radiance from within the field of view of channel 4 was greater than that for channel 3 the star sensor field of view was clear of the earth and its output could be used to control the satellite pitch attitude.

3.2 Optical head

The optical head included the sensor mounting flange and carried 4 plane gold mirrors which determined the orientation of the 4 separate fields of view. These mirrors protruded through the structure of the satellite and directed the 4 optic axes in the satellite pitch plane as previously described. Precise alignment of channel 1 to channel 2 was achieved by adjustment of the entrance mirror on channel 1.

Radiation from within the fields of view was reflected into the sensor along 4 parallel optic axes which were equally spaced on a 40 mm diameter. On each optical axis an $f/4$ germanium lens of 60 mm focal length brought the radiation to a focus on the detector entrance aperture after passage through a short wave pass filter, the modulator and a 14–16 μm band pass filter.

3.3 The IR modulator

The modulator consisted of a gold plated titanium disc with 4 radial slots cut into its circumference. The disc was concentrically mounted on a cross-spring pivot (Bendix type 5016–600) to enable it to oscillate in rotation about its axis. The surface of the disc was spaced 0.5 mm from the band-pass filter attached to each detector. When the disc was at rest the radial edge of each slot was positioned over the centre of each detector field stop and aligned with its major axis. The modulator was maintained in resonant oscillating motion at the design frequency of 116 Hz by an electromagnetic/electronic positive feedback system which drove the modulator with constant current. The drive circuit of the modulator is described in section 3.5 and Appendix B. The amplitude of

oscillation, which was set at 1 mm at the centre of the field stop, was within the "indefinite life" rating of the pivot. A voltage corresponding to modulator amplitude was monitored as part of the sensor housekeeping data and from this it could be seen that the amplitude remained constant to within $\pm 0.7\%$.

3.4 Detector assembly

The detector assembly consisted of a light alloy plate, the centre of which was electrically isolated from the sensor body by an epoxy bond. The detectors were mounted on this isolated section equally spaced on a diameter of 40 mm and in good thermal contact with each other. A thermistor was included on this central plate to monitor the temperature of the detectors.

3.5 The electronic package

The electronic package performed the following functions:

(a) To self-start and run the modulator at constant amplitude and to monitor the modulator amplitude.

(b) To provide the detectors with a low noise dc supply.

(c) To amplify, demodulate and condition the signals produced by the detectors in order to monitor the signal strength from each detector.

(d) To provide a logic signal to the control system to indicate the presence of the earth in, or near, the field of view of the star sensor. This was achieved by comparing the output of channels 3 and 4. To ensure correct operation of this eclipse warning signal remotely commanded gain controls were included in the amplifiers for these channels to enable any excessive differential drift in channel responsivities to be counteracted in orbit.

The circuits of the sensor, and a circuit description are given in Appendix B.

The electronic components were assembled as Multi-Chip-Integrated (MCI) packages by the Plessey Co Ltd. Thick film hybrid circuit techniques developed at RAE for space applications[1] were employed in the manufacture. Seven MCI packages were used as indicated in the block diagram in Fig 8. These were mounted on carriers and assembled into a stack which was mounted behind the detector assembly as shown in Fig 9. The components required for power supply decoupling, RF interference rejection and select on test gain adjustment were mounted on the end and sides of this stack. The decoupling components for the detector supply were mounted below the stack immediately adjacent to the detectors.

4   ALIGNMENT, CALIBRATION AND QUALIFICATION

4.1   Fields of view

The orientation of the fields of view of channels 1 and 2 were adjusted to be parallel in the pitch plane by adjusting the tilt of the mirror on channel 1. This mirror was then dowelled to maintain its alignment. The orientation of the fields of view were determined, relative to two reference mirrors on the optical head, by measuring the polar response of the sensor to a chopped IR line source 8 mm wide at a range of 12 m. The polar response was measured along the major axis and at three positions across the major axis of each field of view. A typical polar response, that of channel 1, is shown in Fig 10. The stability of the sensor fields of view was investigated at temperatures between 20° and 50^oC, and the effect of vibration and thermal excursions was determined by recalibrating the sensor after qualification testing. Results of this work indicated that positions of the fields of view were stable to better than 1 arc minute.

4.2   Radiometric calibration

The output of each channel was dependent on the temperature difference between the sensor and the target viewed by that channel. The gain of each channel was individually set to give an output corresponding to approximately 95% of the telemetry range for the maximum signal condition (sensor at $+30^oC$ and viewing space).

The sensor was then calibrated as a radiometer by placing the instrument in an isothermal temperature controlled jacket, within a vacuum chamber, so that each field of view was directed into a conical black body. The two independent variables, sensor temperature and black body temperature were then adjusted over their appropriate ranges to produce the calibration chart of Fig 11. At constant sensor temperature there is a linear relationship between the output of each channel and the spectral radiance of a black body filling the field of view of that channel. A family of curves, for a range of sensor temperatures, was therefore obtained by determining two points on each curve viz, the channel output for zero black body radiance and the black body radiance required to produce zero AC output from the detector.

The calibration plan adopted, illustrated in the visit of Fig 11, was as follows:

(i)   Step 1 (A to B) with the black body temperature constant at 77K
($\approx$ zero radiance) the channel outputs were continuously measured
as the sensor temperature was reduced from 305K to 265K at 2K min^{-1}.

(ii) Step 2 (B to C) with the sensor temperature constant at 265K the
black body temperature was raised to 271K.

(iii) Step 3 (C to D) the sensor temperature was raised continuously at
0.2K min^{-1} and the black body temperature was raised in 4K steps
providing a series of calibration points when both the sensor output
was zero and the black body temperature was constant.

In this way an absolute calibration of the sensor was obtained over its operating
temperature range with an estimated probable error of 3%.

It was found during calibration that, despite previous screening, the
sensitivity of channel 2 was beginning to exhibit variations of the type
associated with thermally induced noise. However, due to the timescale and the
then current state of the detector development, it was decided to accept it.

4.3   Spectral response

The spectral transmissions of the optical components were measured by the
manufacturers, Sir Howard Grubb Parsons Ltd, a typical cascaded transmission
curve, that of channel 1, is reproduced in Fig 12.

4.4   Sensor qualification

Three IR sensors, a qualification model, flight model and flight spare
were delivered to HSD Ltd for assembly, integration and test in the satellite
structure. These sensors had previously been subjected to a series of tests
outlined in HSD document DHMT 13146 – Environmental Test Specification for Units.
The qualification model was subjected to test levels more stringent than the
anticipated Scout launch environment in order to reveal any deficiencies in the
sensor design. The flight sensor test levels were less severe and intended to
reveal material or workmanship defects in the flight unit.

5   EXPERIMENTAL RESULTS

5.1   Data transmission

Data obtained during each orbit (101.2 mins) was recorded on the satellite
tape recorder and played back on command from the ground station at Lasham

England. In addition direct data were received during short periods before and after the tape recorder replay. The telemetry channel allocation and sampling rates are shown in Table 1.

5.2 Detector performance

5.2.1 Responsivity

The stability of the detector responsivities was monitored for each channel separately, and for channels 1 and 2 as a differential pair this was done by comparing the channel outputs when each field of view was directed at space (zero radiance) with the values in the preflight calibration at the same sensor temperature. The results of this comparison are shown in Fig 13. Channel 1 can be seen to have performed perfectly throughout the 270 days of monitored flight with no perceptible change in its sensitivity. Its absolute sensitivity was measured as approximately 2% higher than that determined prior to launch. Channel 2 also started its life 2% above the prelaunch calibration level and remained btween 2 and 4% above this value for most of the first 200 days, only occasionally dropping 5 or 10% for isolated periods just after launch and again after about 90 days. From 200 days after launch the mean level of indicated sensitivity dropped 10% to 15% and showed fairly large variations. From our previous experience of these detectors this was thought to be due to thermally induced noise. Channels 3 and 4 also showed sensitivity variations throughout the spacecraft's life and these were considered to be again indicative of the presence of thermally induced noise.

5.2.2 Noise

It was not possible to make precise measurements of detector noise in orbit. However estimates of the noise could be made by monitoring the output of each channel during the periods when the signal was constant ie when it was observing space.

There was no detectable change in the noise level measured in channel 1 (1 telemetry bit $\approx$ 1σ) but thermally induced noise prevented meaningful estimates of the noise in the other channels.

5.3 Attitude measurement

Channel 1 of the IR experiment was used as the primary pitch attitude sensor throughout the life of the satellite. An attitude determination routine was constructed to recognise the instant at which the output signal of

channel 1, which changed rapidly as the field of view of the channel crossed the horizon, was midway between the steady values on either side of this change.

At these instants the centre of the field of view was assumed to be tangential to a spheroid 40 km above the earth sea level spheroid. A more complete description of the processing of this data can be found in reference 2, which also reports agreement between the gyroscopes and the sensor attitude measurements of typically 0.06 degrees (1σ) over periods of up to two days. Further study of the results shows that this could be improved to a figure of 0.03 degrees (1σ) by increasing the reference spheroid altitude to 43 km above sea level and this value was adopted in the attitude determination programme used for the earth radiance analysis.

5.4   Earth radiance measurements

Having radiometrically calibrated the experiment prior to launch and checked this calibration frequently in orbit, using space as the reference, channel 1 of the sensor was used to measure the radiance of the earth in the 14 to 16 μm spectral region. At intervals of approximately 14 days the satellite pitch rate was held constant at 25° per hour for periods of two to three days, during this time the sensor was able to observe the earth at all latitudes from about 80° North to 80° South.

The latitude and longitude of the intersection of the centre of the field of view of channel 1 with the surface of the earth was determined for each data point from that channel. The angle of elevation of the line of sight at the earth surface was also calculated. Mean values, and the standard deviation of earth radiance were then obtained as a function of latitude alone. Data were used only when the angle of elevation of the line of sight exceeded 25°. The angle of longitude over which data was available was limited to two sectors of about 60° centred on longitudes 0° and 180° by the siting of the single ground station used for reception of the telemetry data. A selection of results, corresponding to approximately monthly intervals from March to November 1974, is given in figs 14 to 23. It should be noted that the value of radiance given is the spectral radiance at 15 μm of an equivalent black body target which completely fills the field of view of the instrument.

The standard deviation of the radiance measurements is generally small indicating that other factors such as longitude have a relatively minor effect on the radiance. However there are periods when this is not so and to

illustrate the variations found in such periods the details of radiance data collected between 20° South and 80° South for the period from the first morning pass (M1) on 10 September to the last evening pass (E3) on 11 September are given in Fig 24. This figure includes well over 80% of the data used to compile the mean radiance curve shown in Fig 20.

The data was collected during the three morning and three evening orbits received on 10 September and two of the morning and one of the evening orbits received on 11 September. The areas of the earth observed during these orbits is shown in Fig 25 which also shows the path of the sensor field of view on the earth. The times of the observations in these selected orbits are given below:

10 September	M1	01:20:37	to	01:46:45	GMT
"	M2	02:55:53	to	03:19:21	
"	M3	04:35:24	to	04:46:28	
"	E1	14:56:12	to	15:20:28	
"	E2	16:27:20	to	16:53:28	
"	E3	18:06:06	to	18:20:38	
11 September	M1	03:02:25	to	03:11:29	
	M2	04:32:56	to	04:51:20	
	E3	18:09:06	to	18:21:54	

It will be seen from Figs 24 and 25 that the radiance pattern is relatively stable with respect to time over this period but that there is a marked rise in the radiance in the region around 30° East, 55° South and it is this that has given rise to the large standard deviation recorded in Fig 20.

6   DISCUSSION OF RESULTS

6.1   Detector performance

The self calibrating nature of the experiment, and the use of four detectors all sharing common conditions gave a high degree of confidence in the observations made. As preflight study had shown, there was a high probability of the occurrence of thermally induced noise in one or more detectors occurring during the mission. Channels 2, 3 and 4 showed characteristics indicative of this type of phenomenon but fortunately the channel used for measuring the earth's radiance, channel 1, was fitted with a detector that functioned perfectly throughout the spacecraft's life. The conclusions to be drawn from the evidence gathered in orbit and in the laboratory prior to launch, are that it is possible to construct reasonably robust detectors which give consistent and good

performance. However the TGS material must be processed with extreme care, particular regard being paid to its tendency to absorb water. Furthermore the packaging must ensure that the detector element is maintained in a suitable environment throughout its operating life. The detector manufacturer has stated that by observing these principles success has been achieved in obviating the noise failure mechanism.

6.2 Modulator performance

The resonant oscillatory modulator used in this experiment performed admirably throughout the life of the experiment maintaining an amplitude stability of better than $\pm0.7\%$ with constant current drive to its excitation coils.

6.3 Earth radiance measurements

The preceding sections of this paper describe the instrument used for the radiance measurements and the techniques used to ensure the validity of the results. The in-orbit calibration, as summarised in Fig 13, indicates that the measurements made using channel 1 of the radiometer can be regarded with a high degree of confidence. The main interest in these radiance measurements is for application to the design of horizon sensors for earth referenced spacecraft. Inspection of Figs 14-23 reveals that the gradient of radiance with respect to latitude can at times be quite steep. This is a parameter which in the past has often been represented by more simple models which could lead to inadequacy of sensor design. Although it is not known if this data is typical it is suggested that sensors should be designed to accept radiance patterns at least as demanding as those shown here. The expansion of Fig 20 into its component data, as shown in Figs 24 and 25, reveals that in some areas the radiance variations are particularly severe. To illustrate this Fig 26 has been constructed from the data obtained during orbit E1 of 10 September. This demonstrates the variation in radiance profile that could be encountered by a North-South scanning instrument in a satellite at geosynchronous altitude.

Finally it should be emphasised that the local variations with longitude, as described in section 5.4 and reported elsewhere[3], imply that East-West scanning instruments should also be designed to cope with fairly steep radiance variations in the vicinity of the horizons.

14

Appendix A

OUTLINE SPECIFICATION OF P200X DETECTOR

Type of detector	Pyro-electric infra-red detector, incorporating a light-pipe and germanium field lens bloomed for maximum transmission at 15 μm.
Sensitive material	Deuterated, Aniline doped, Triglycine Sulphate.
Sensitive area	0.55 mm x 0.55 mm.
Entrance aperture	3 mm x 1 mm.
Field of view	$\pm 8^\circ$ nominal.
Cooling	None.
Number of elements	One.
Envelope	Metal case, epoxy sealed.
Type number	P200X.
Operating voltage	10 volts nominal.
Responsivity at 20°C (500K: 90)	5×10^3 VW^{-1}.
NEP at 20°C (500K: 90 : 1)	5×10^{-10} WH$_2^{-\frac{1}{2}}$.
Operating temperature range	-20°C to $+50^\circ$C.

Appendix B

ELECTRONIC CIRCUIT DESCRIPTION

B.1   The modulator

The circuitry associated with the modulator, shown in Fig 27 was mounted in one MCI package, designated IS3. The signal from the pick-off coil of the modulator is amplified and then fed into a high gain amplifier which saturates and thus feeds the modulator drive coils with a constant current amplitude square wave. It is important to note, that despite the fact that the amplifier is used in a saturating mode to run the modulator, it is necessary to bias it into a linear mode to enable the device to be self starting. The amplitude of the modulator pick-off signal is measured by device A4, the output of which was telemetered in order to monitor the modulator behaviour. Finally, amplifier A3 provides a reference signal to the six phase sensitive detectors in the signal channels.

B.2   The signal channels

Signals from each detector are fed into separate processing channels, each contained in a separate MCI package, all designated IS1 and illustrated in Fig 28. The voltage gain of the first stage A1 is in the region of 100, and was adjusted using the AOT resistor to accommodate the detector responsivity. The frequency response up to the phase sensitive detectors extended from 12 Hz to 4 kHz to make the phase shift of the signal insensitive to component tolerances. The ultimate bandwidth of the processed signal was limited to approximately 0.5 Hz by the low pass filter following the phase sensitive detector. Signals from each pair of detectors were differenced after the first stage of amplification and then processed using phase sensitive detectors and low pass filters and telemetered. The differencing and processing circuitry for each pair of channels was contained within separate MCI packages, designated IS2, and the circuits for these are illustrated in Fig 29. The eclipse warning logic signal, generated to indicate when the star sensor field of view was near the earth, was obtained by triggering the threshold detector (device A4 of IS2) from the difference signal, channel 4-3. The setting of this threshold level, its hysteresis, and the relative gains of channels 3 and 4 were mutually optimised to permit up to $\pm 8\%$ drift in the responsivities of detector 3 or 4 without affecting the operation of the eclipse warning system. Further drift in detector responsivities could be accommodated by commandable gain changes in the first

stage of these channels. There were 4 gain settings for each channel, 81%, 86%, 93% and 100% of maximum, and these changes were achieved by short circuit of the feedback around the first amplifier of channels 3 and 4 using the switches TR1 and TR2.

Careful attention was paid to the decoupling requirements of the experiment. The power supply lines were RF decoupled using an L—C network tuned to the satellite's telemetry frequency. Further LF decoupling was achieved by using redundant quads of tantalum capacitors on each power line, and finally the power supply for each detector was separately decoupled by a transistor buffered RC smoothing circuit.

Table 1

TELEMETRY USED FOR X4 EXPERIMENT B DATA CHANNELS

Parameter	Channel Type	Frame Major	Frame Minor	Sampling interval Direct data	Sampling interval Recorded data
Infra-red detector 1	Analogue	077	all	0.25 s	8 s
Infra-red detector 1	Analogue	177	all	0.25	8
Infra-red detector 2	Analogue	147	1.3.5.7	1	32
Detector 2-Detector 1	Analogue	147	0.2.4.6	1	32
Infra-red detector 3	Analogue	045	0.4	2	64
Infra-red detector 4	Analogue	045	1.5	2	64
Detector 4-Detector 3	Analogue	143	2	4	128
Detector assembly, temperature	Analogue	45	2	4	128
Optical head, temperature	Analogue	45	3	4	128
Chopper amplitude	Analogue	45	6	4	128
Star sensor eclipse warning	Digital	105	bits 1.2	0.5	16
Detector 3 gain	Digital	105	bits 3.5.6	0.5	16
Detector 4 gain	Digital	105	bits 4.7.8	0.5	16

Resolution 1 part in 256 on all analogue channels

The data format is described more fully in HSD, Specification – Operations Requirements. DHM (REQ) 12637

REFERENCES

No	Author	Title, etc
1	D. W. Allen J. A. C. Beattie P. Clarkson	Multichip integrated circuits in UK spacecraft. RAE Technical Report 75038 (1975)
2	W. G. Hughes	Operational experience of the Miranda (X4) satellite attitude control system. RAE Technical Report 75116 (1975)
3	J. J. Barnett	Large sudden warning in the Southern hemisphere. Nature Vol 255 pp 387-389 29 May 1975
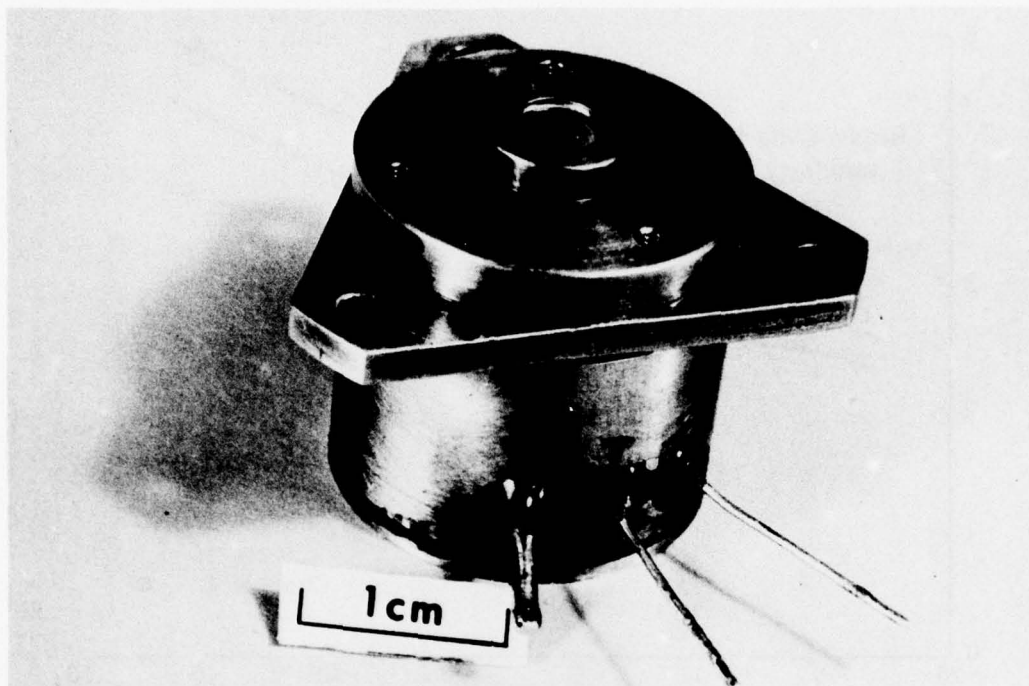
Fig 1　The P200X detector

Output voltage mV
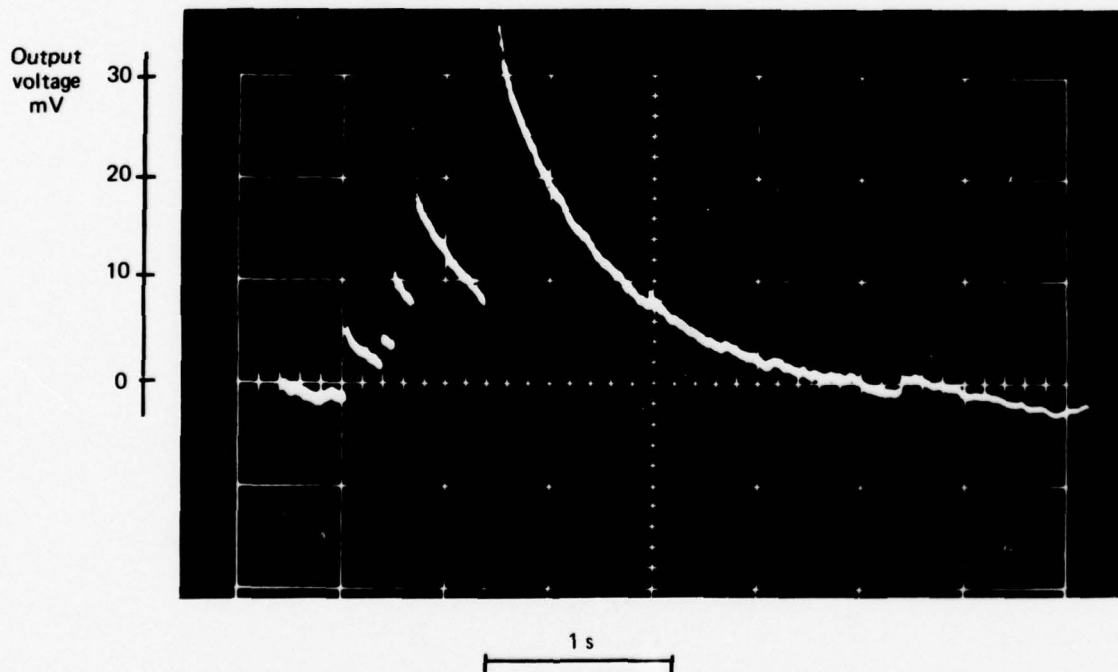
Fig 2　Thermally induced transients from a P200X detector
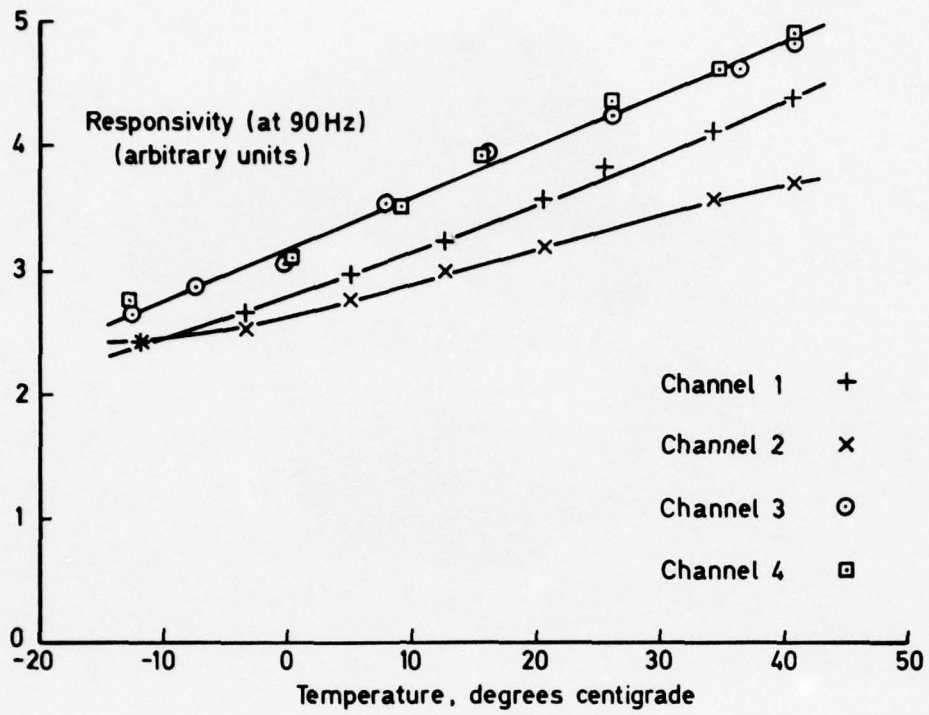
Fig 3   Responsivity of flight detectors versus temperature
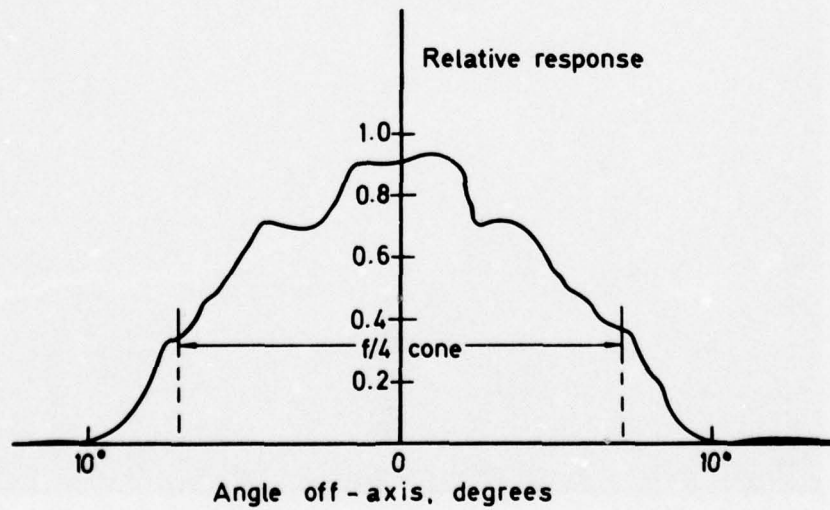
Fig 4   Polar response of detector used in channel 1
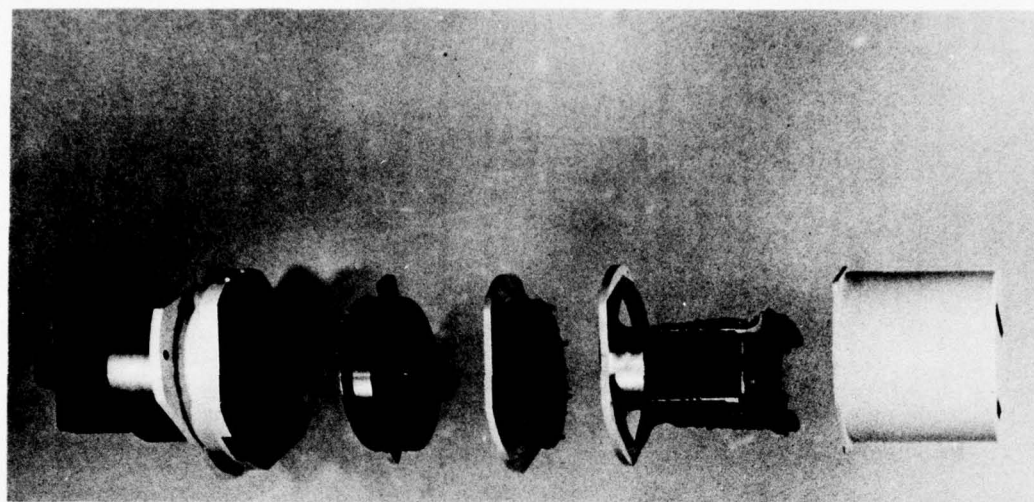
TR 77161

Optical head   Modulator   Detector
assembly   Electronic
package   Cover

Fig 5   Exploded view of sensor

3 cm
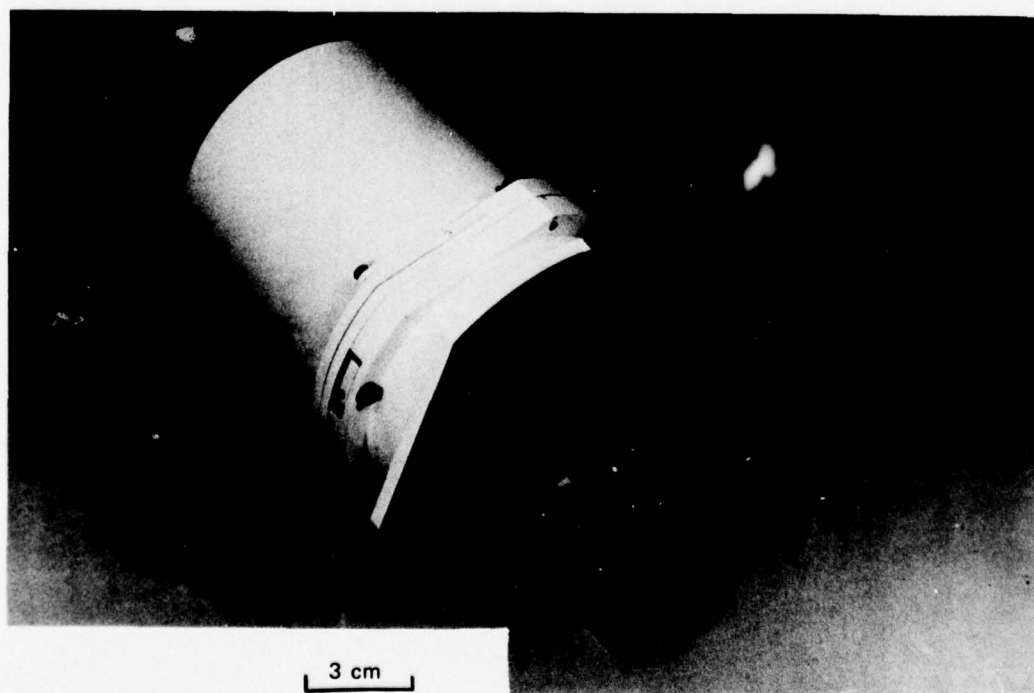
Fig 6   X-4 infrared sensor

TR 77161 C14570
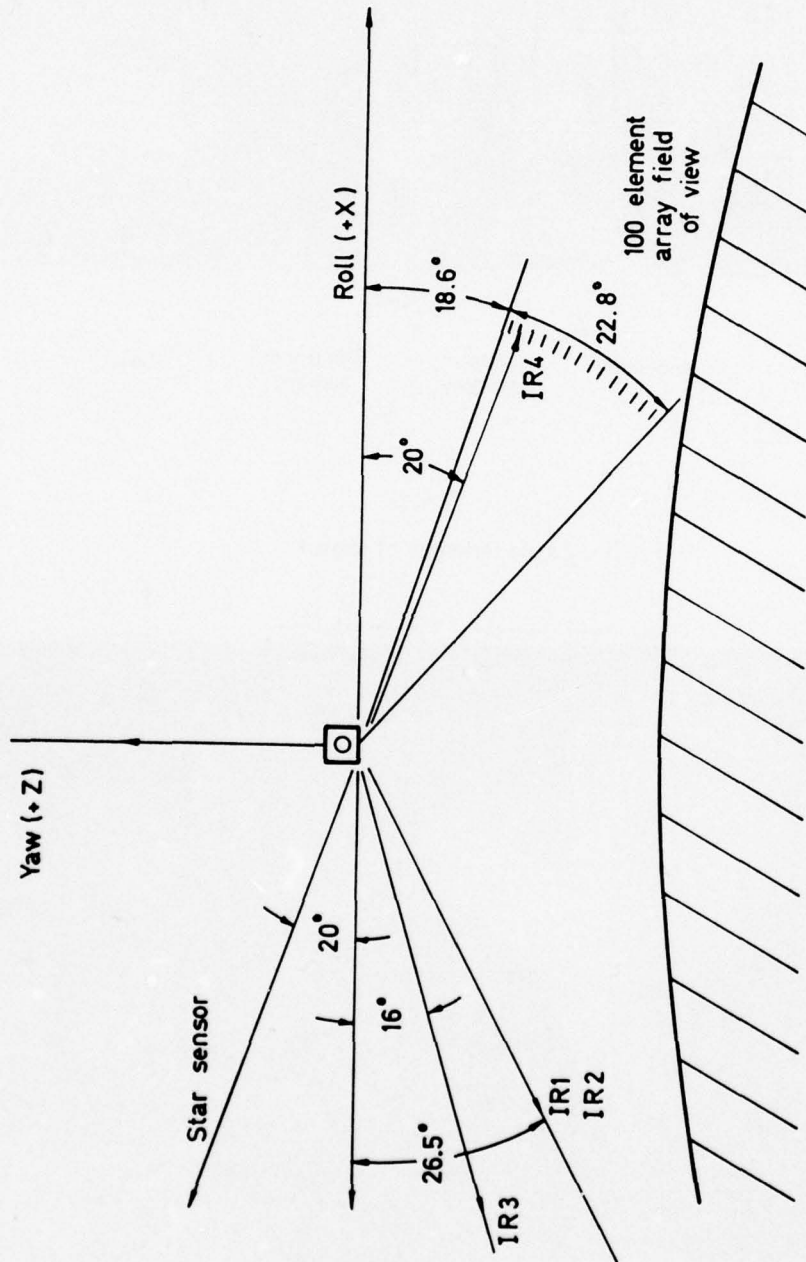
Fig 7

Fig 7   Miranda experimental sensors fields of view

TR 77161
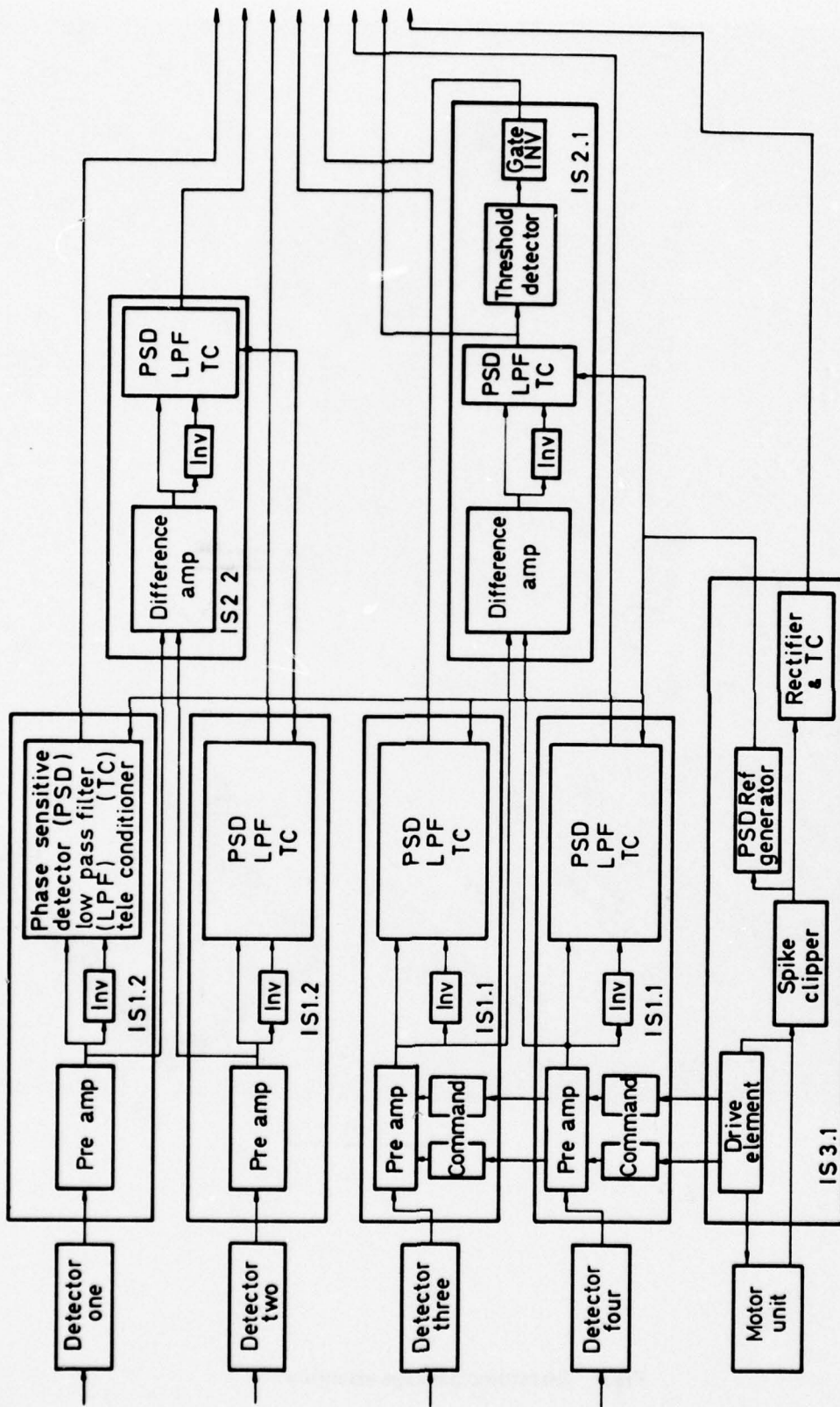
Fig 8

Fig 8   Block diagram of sensor electronics

TR 77161

Fig 9

3 cm
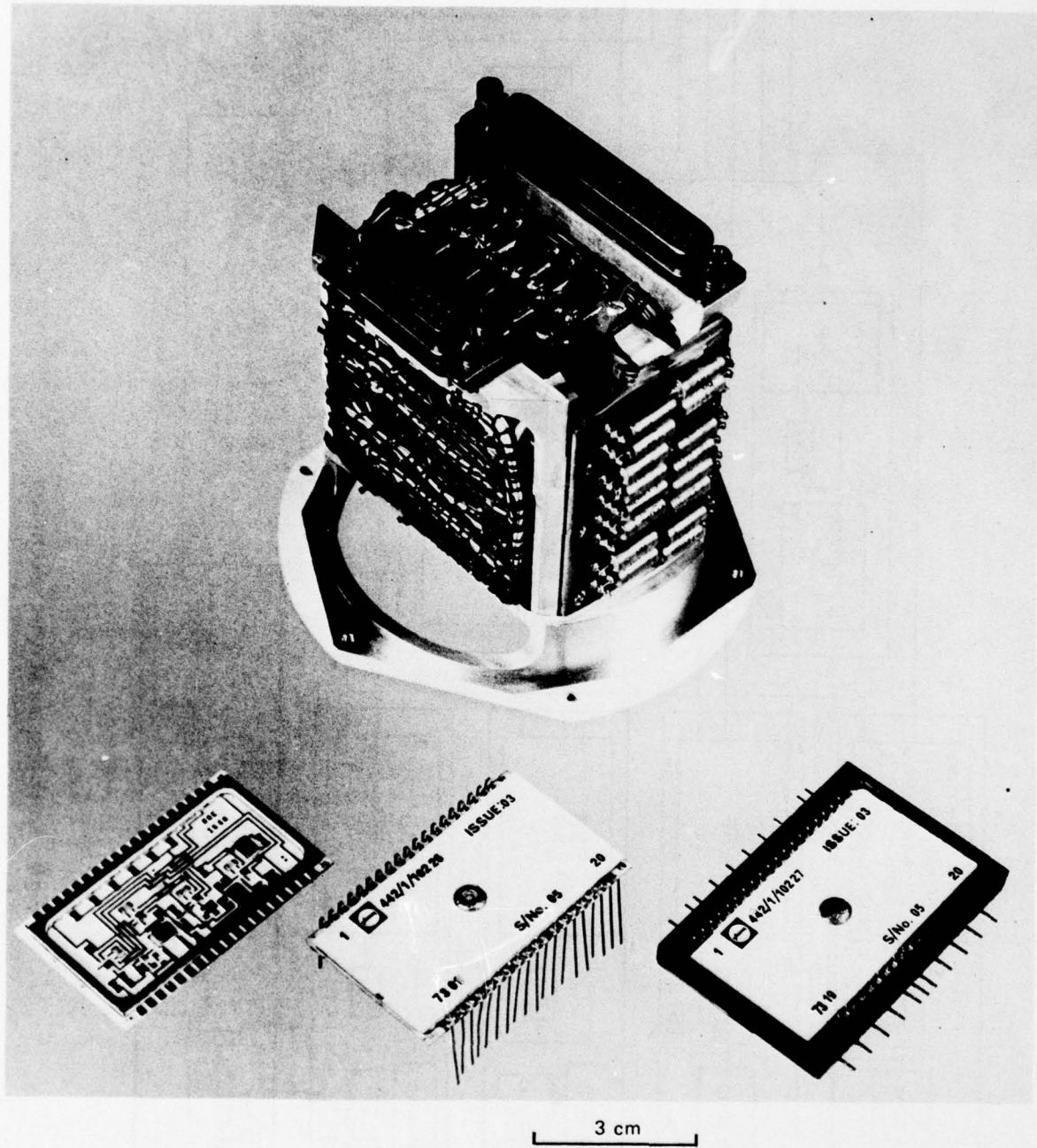
Fig 9   Electronic package assembly
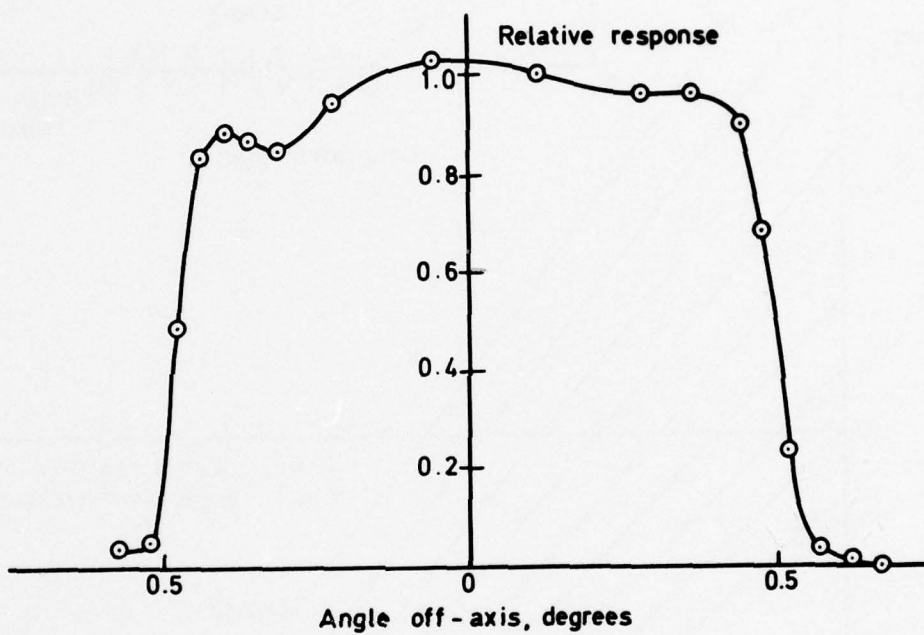
Fig 10

Fig 10   Polar response of channel 1

Fig 11
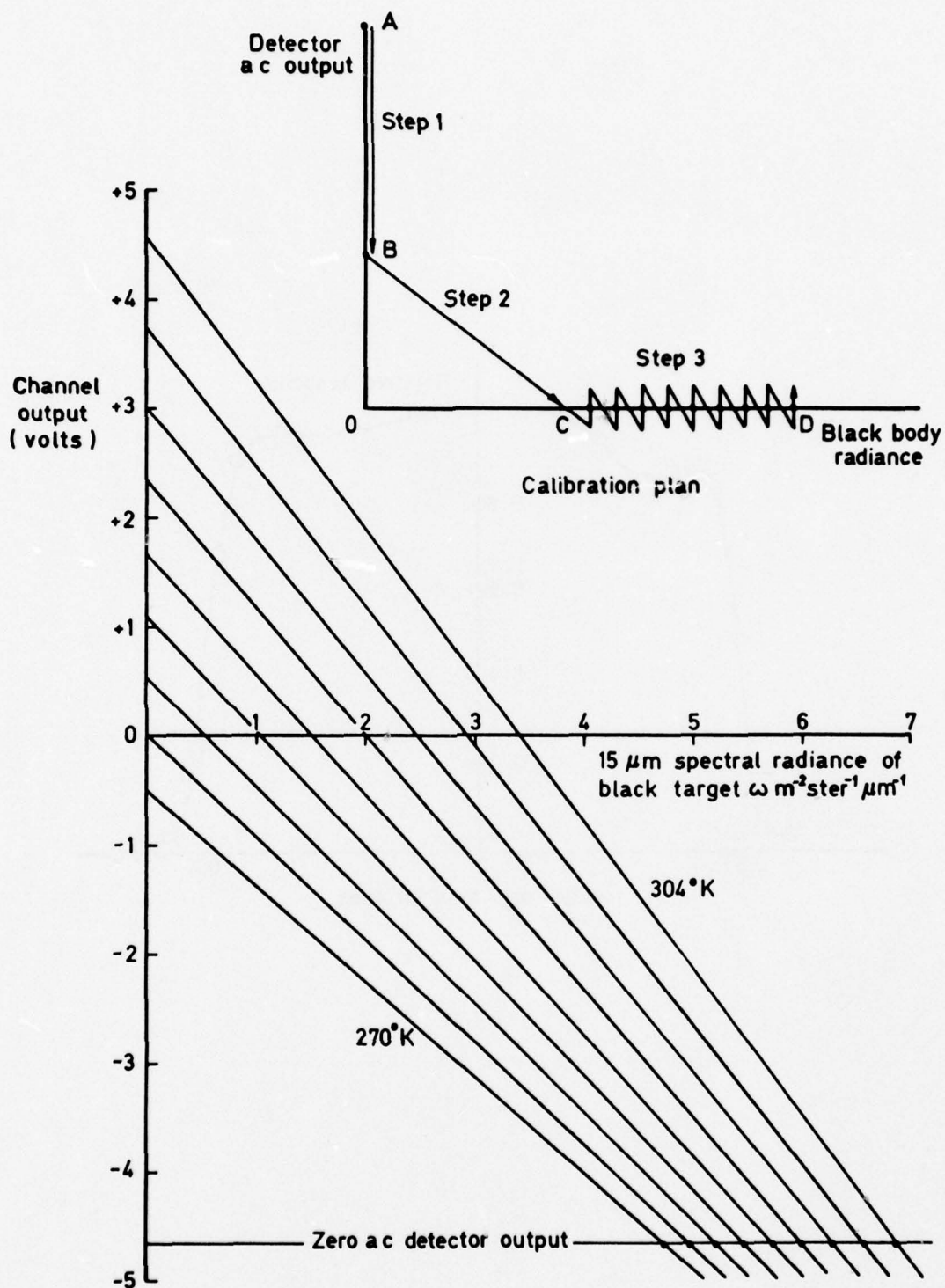
Fig 11   Radiometric calibration and calibration plan

TR 77161
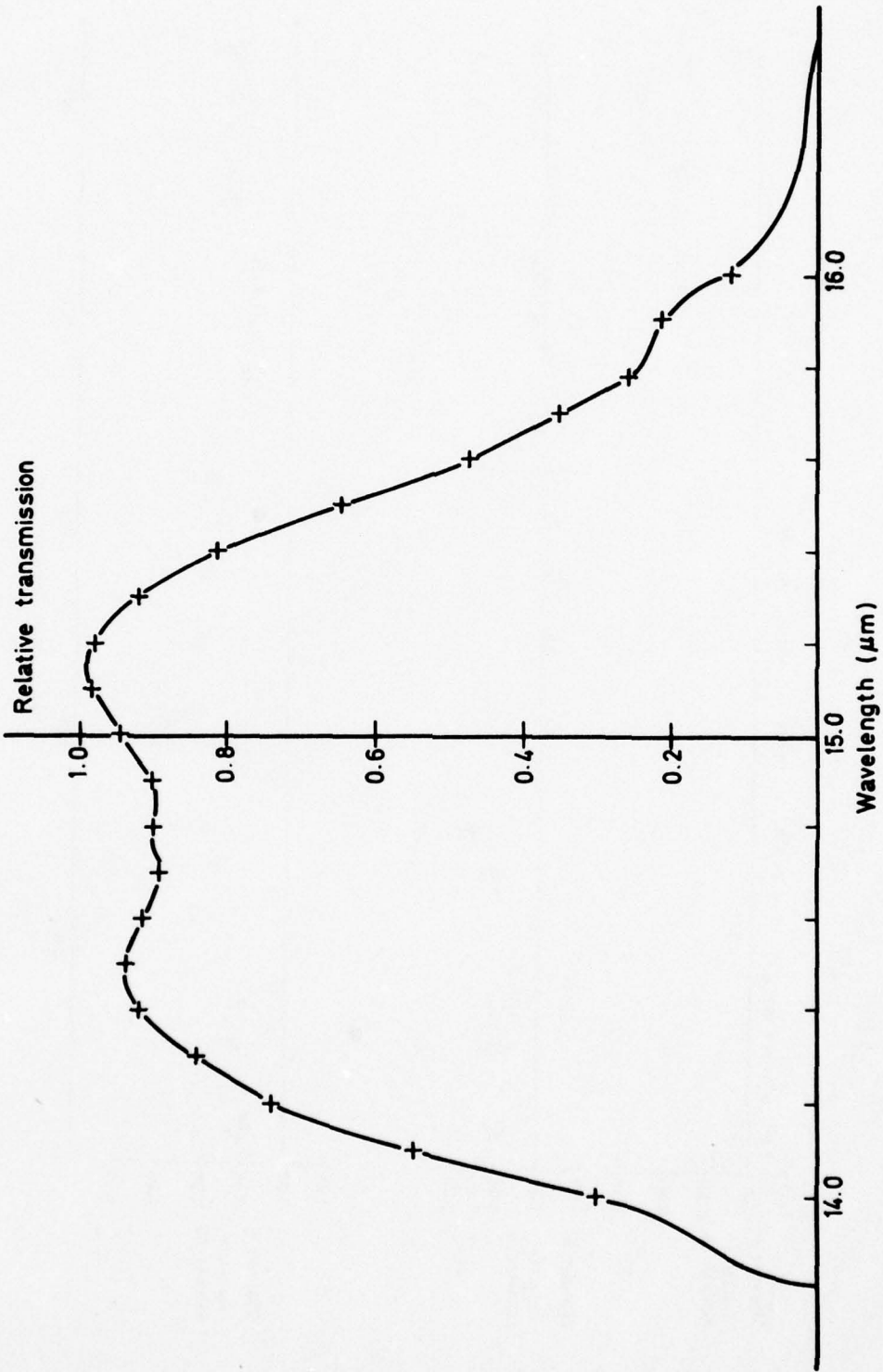
Fig 12

Fig 12   Cascaded spectral transmission of channel 1 filters

Fig 13
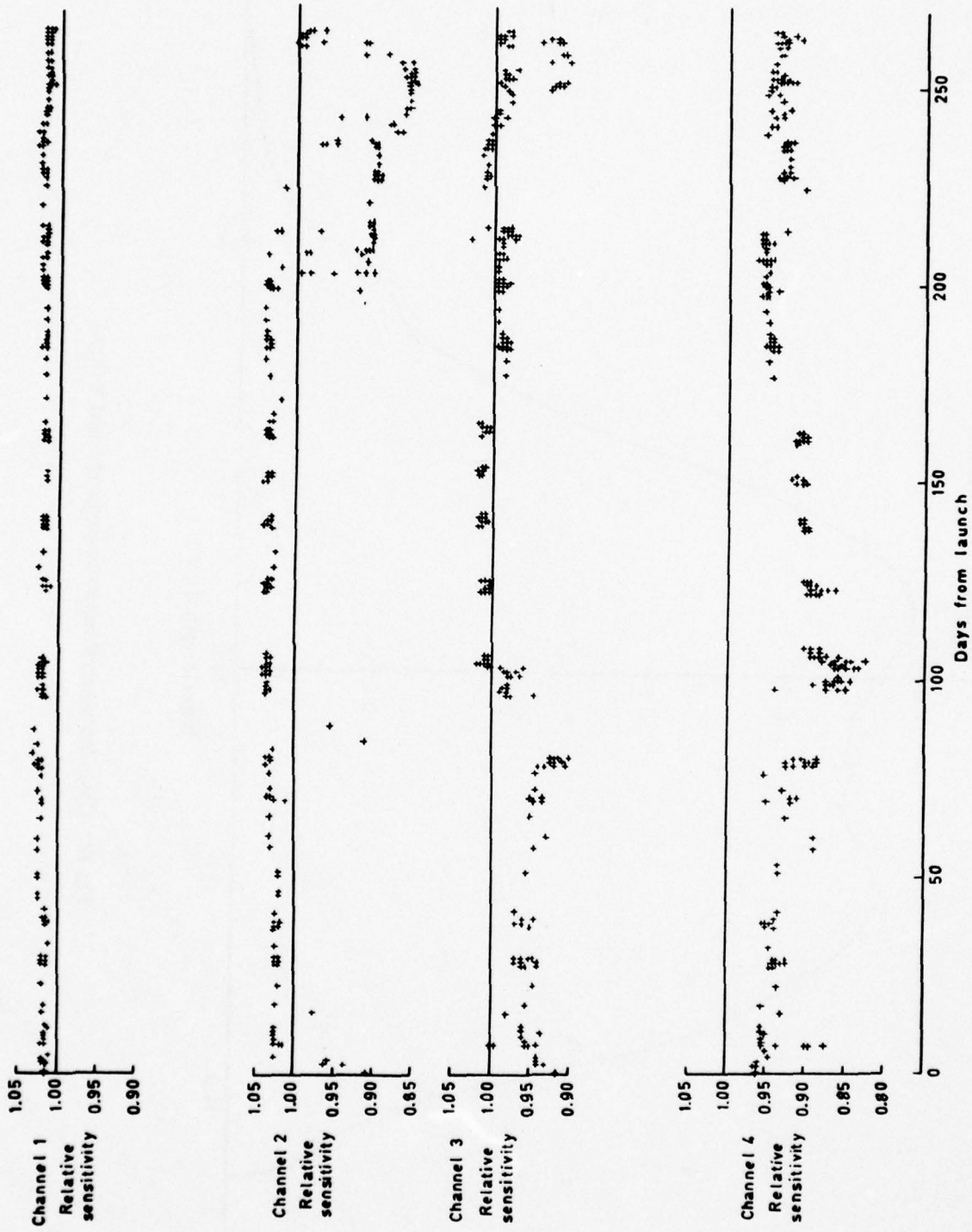
Fig 13   Channel sensitivity relative to pre-launch value throughout spacecraft life
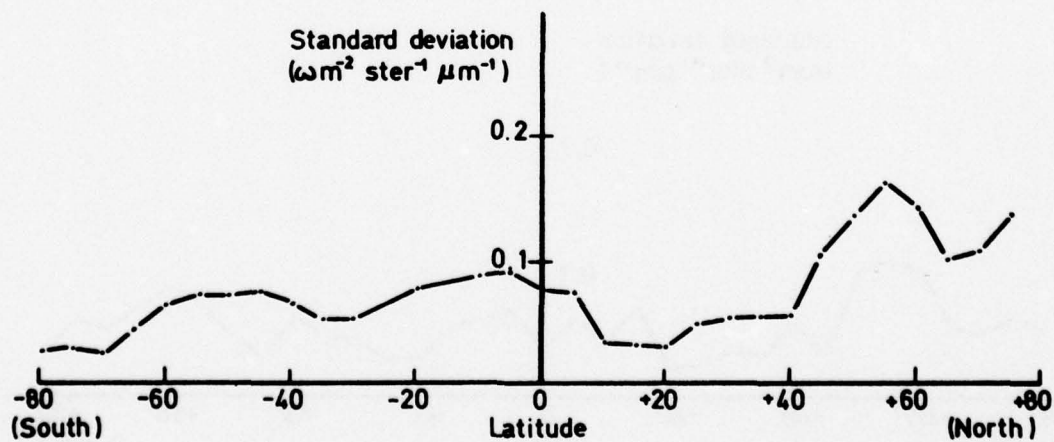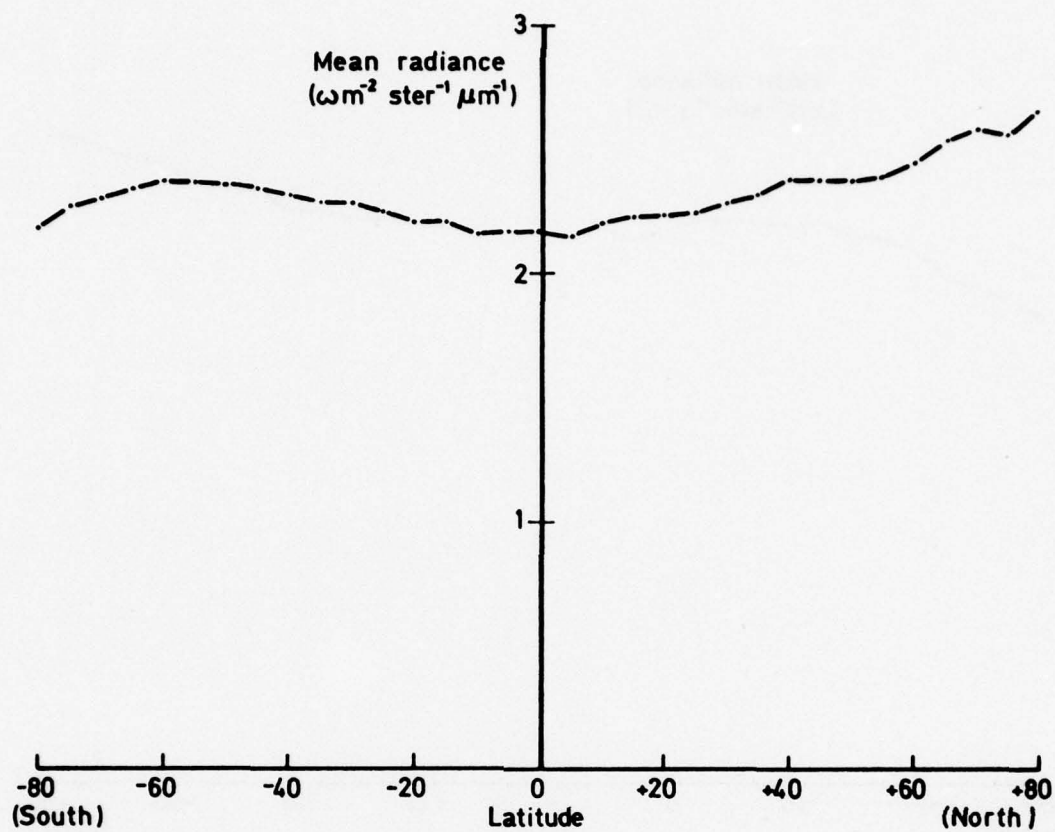
Fig 14

Fig 14   Earth radiance — 26-28 March 1974

Fig 15

Mean radiance
$(\omega m^{-2} ster^{-1} \mu m^{-1})$

3

2

1

-80 (South)   -60   -40   -20   0   +20   +40   +60   +80 (North)

Latitude

Standard deviation
$(\omega m^{-2} ster^{-1} \mu m^{-1})$

0.2

0.1

-80 (South)   -60   -40   -20   0   +20   +40   +60   +80 (North)

Latitude
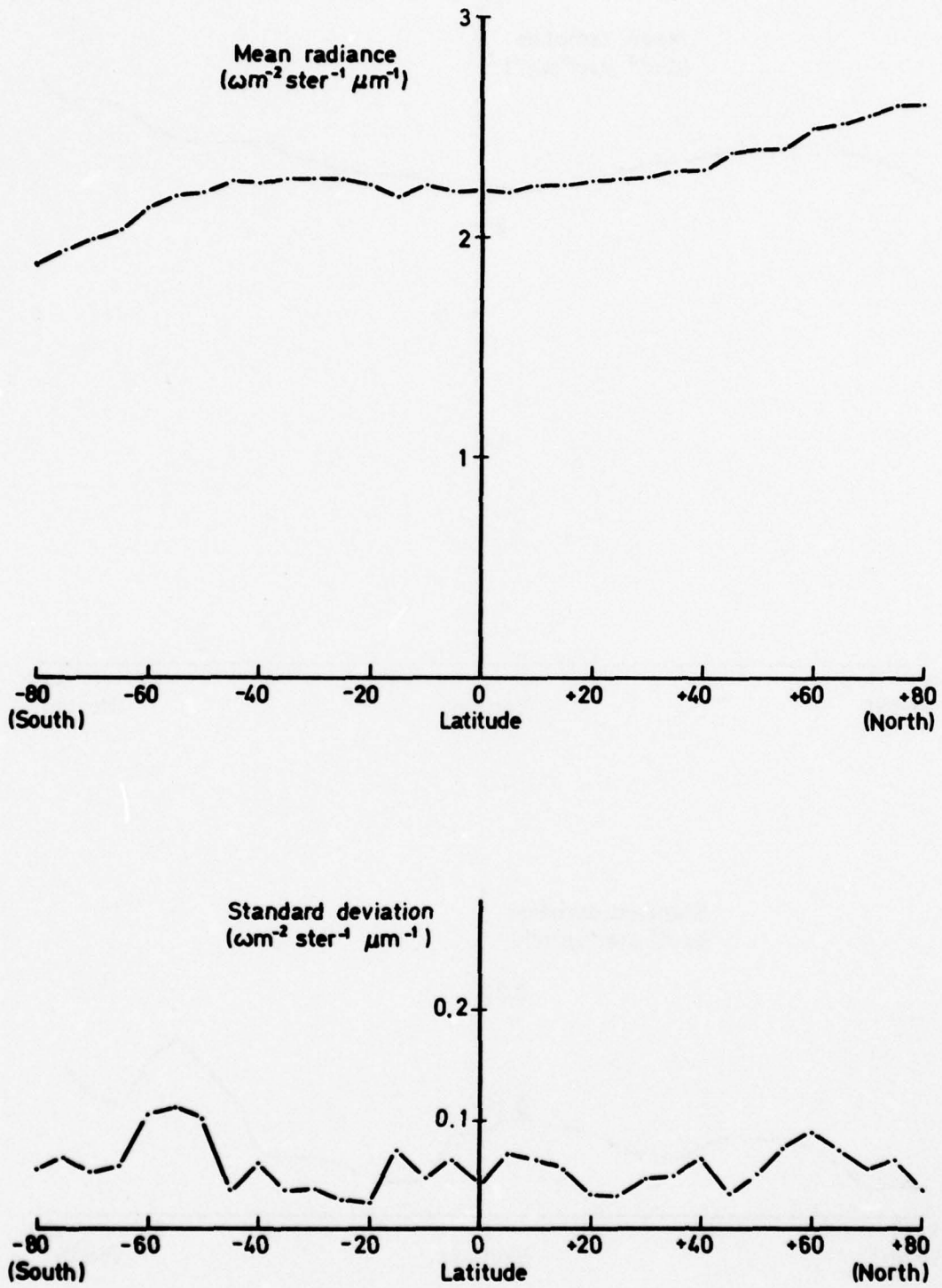
Fig 15   Earth radiance — 15-17 April 1974
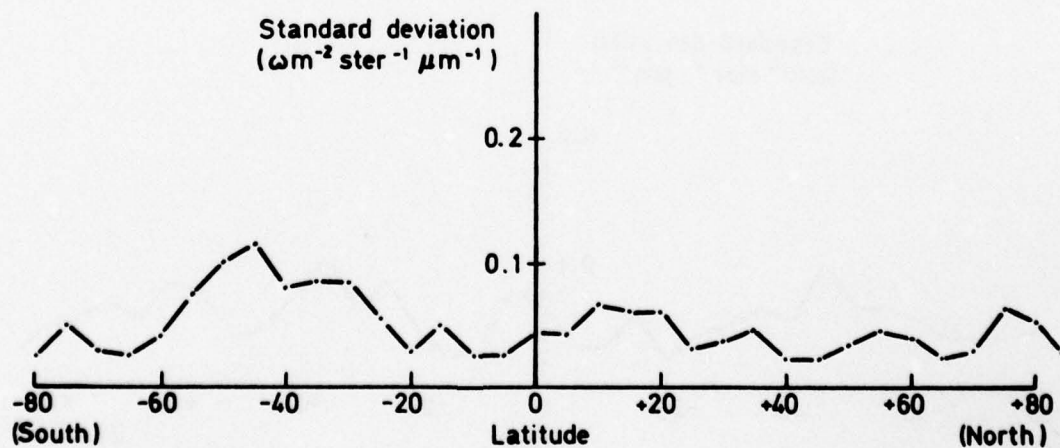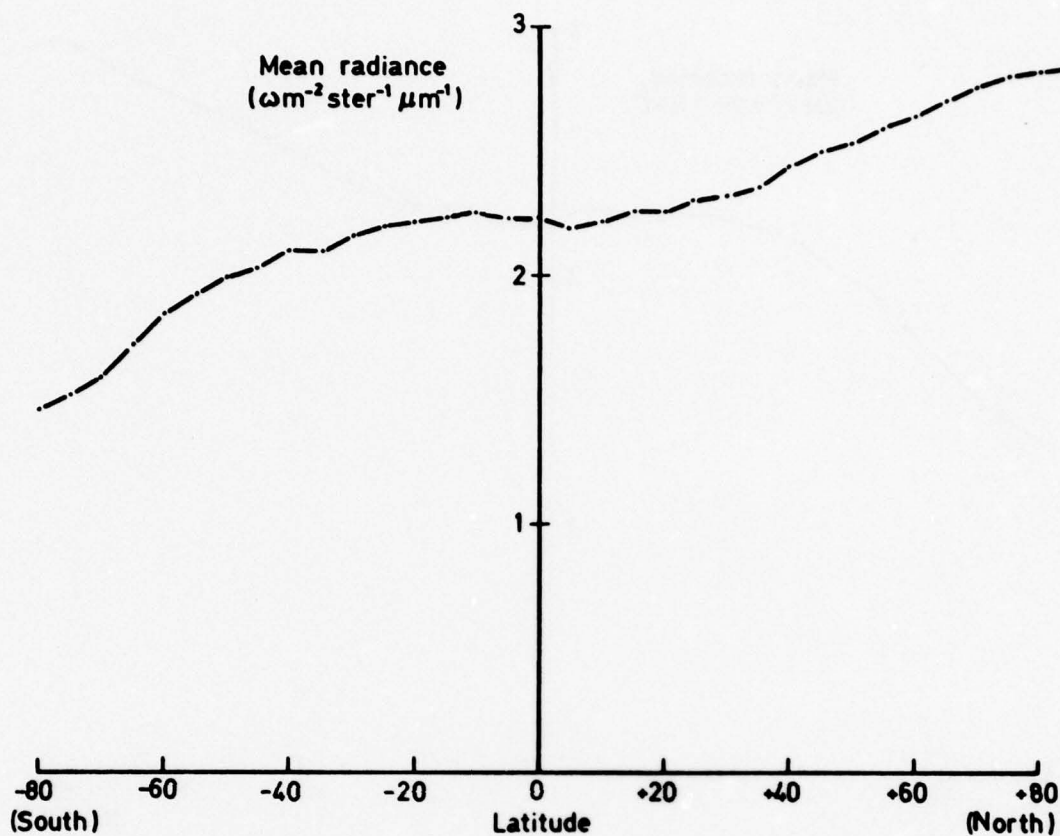
TR 77161

Fig 16

Fig 16   Earth radiance — 26-28 May 1974
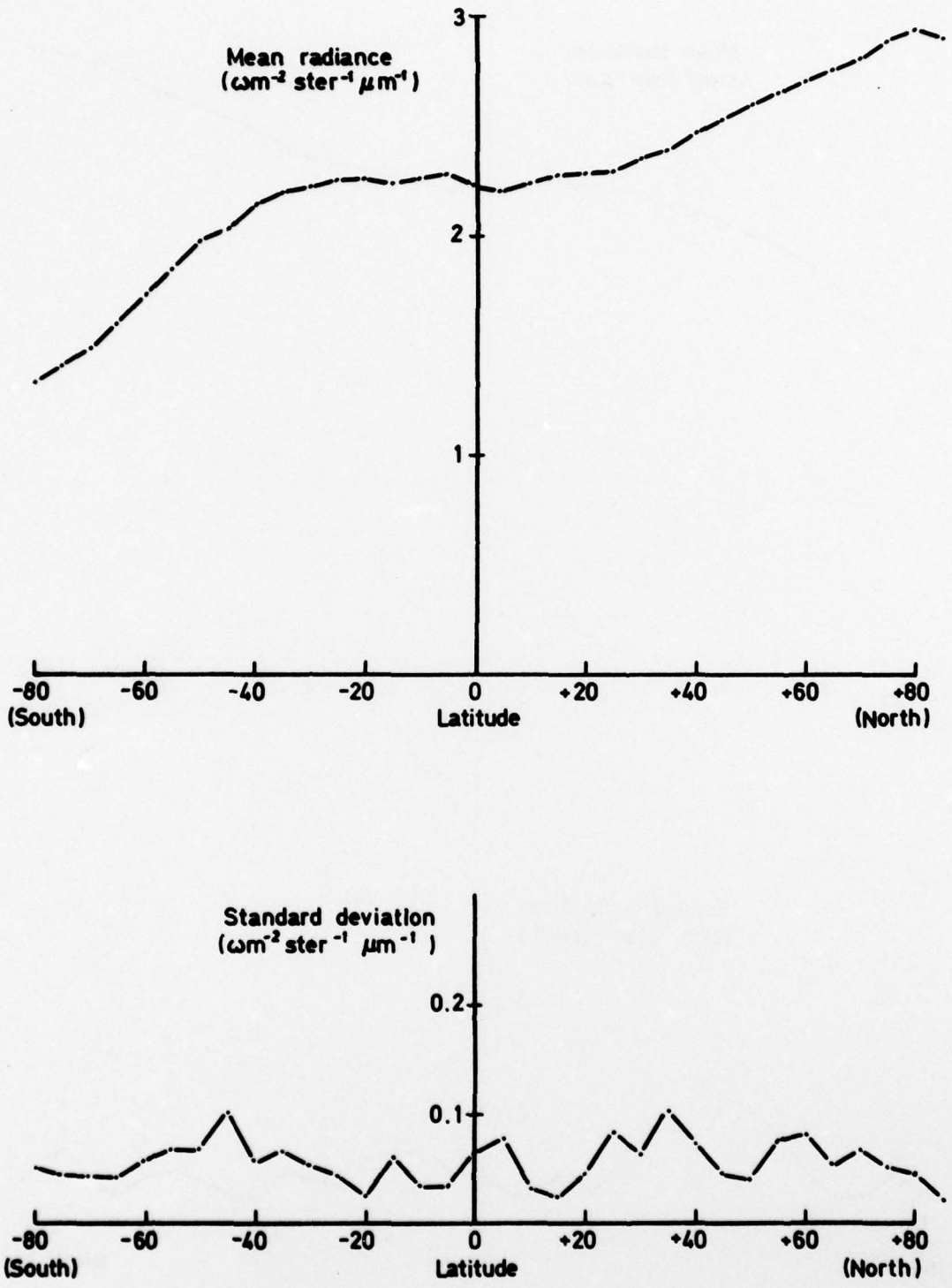
Fig 17

Fig 17   Earth radiance — 18-20 June 1974
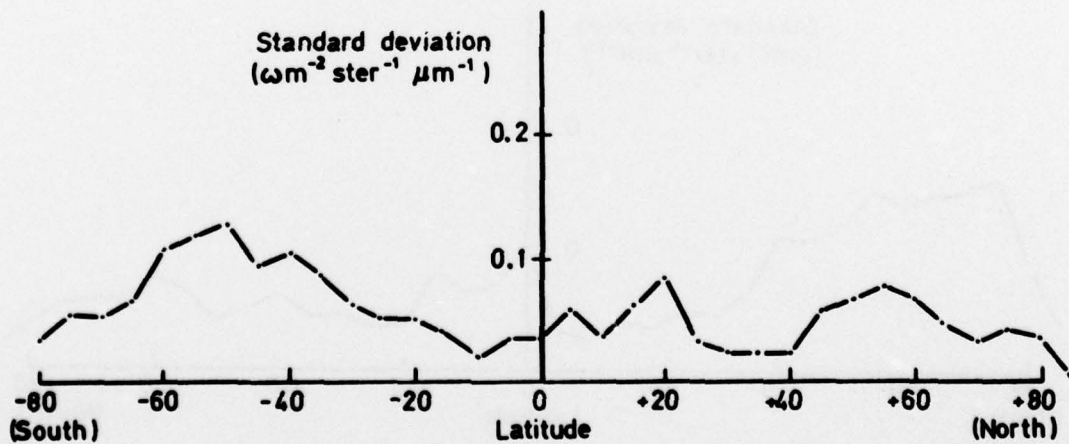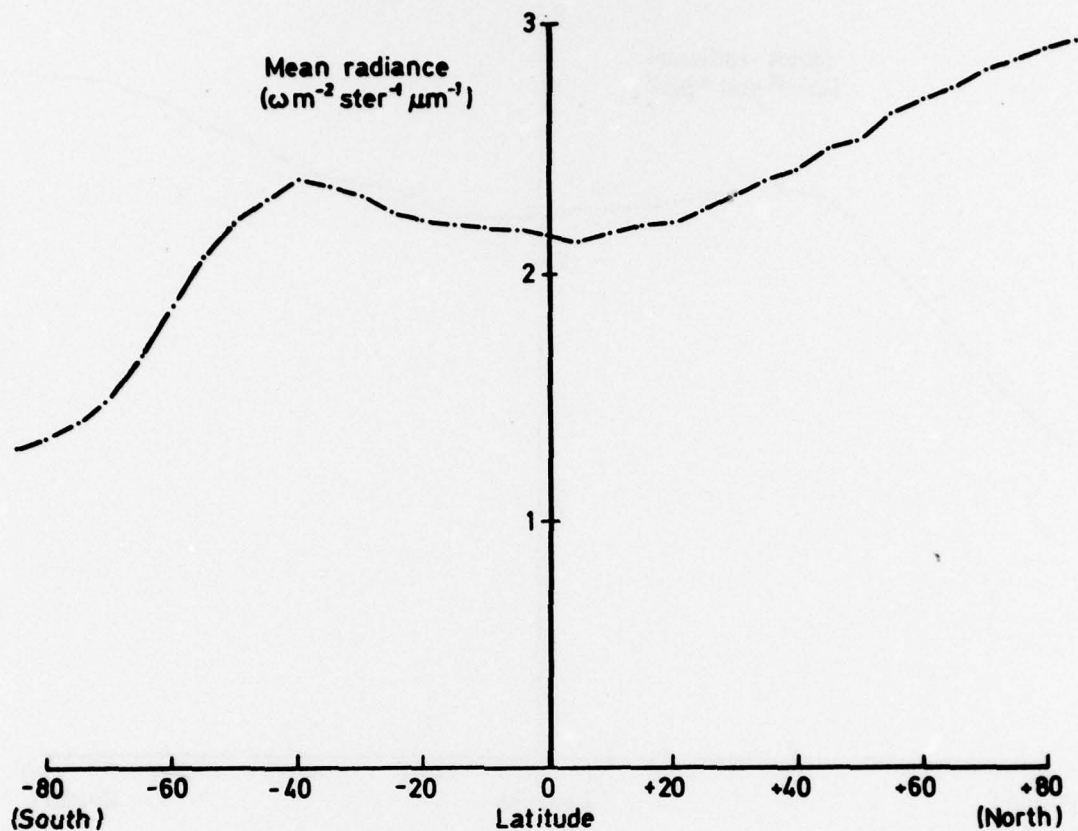
Fig 18

Fig 18   Earth radiance — 25-28 July 1974

Fig 19
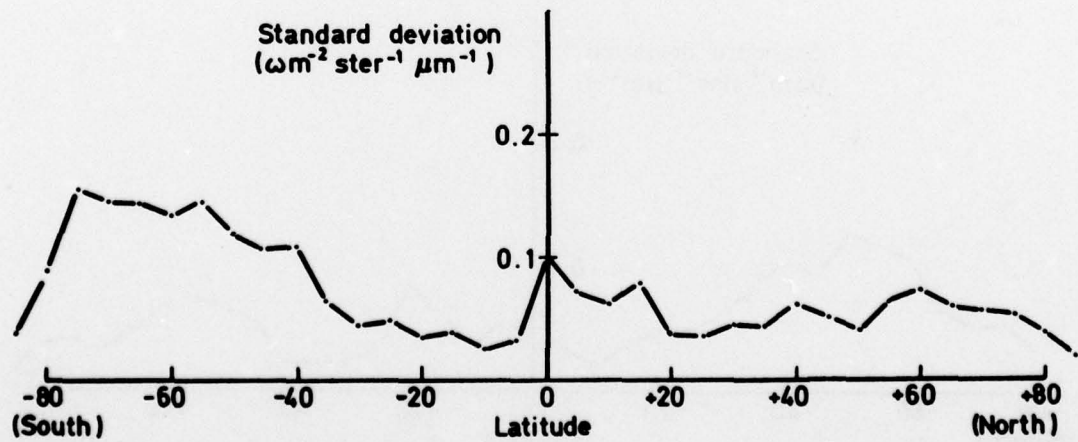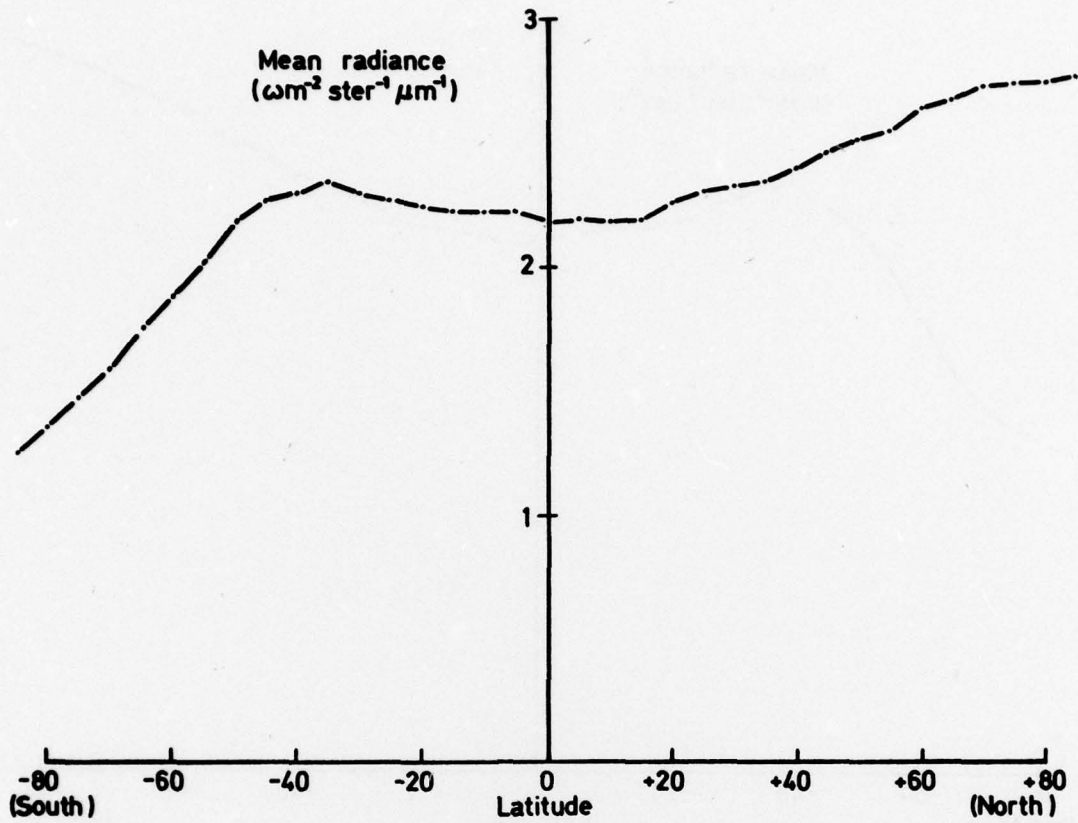
Fig 19   Earth radiance — 16-19 August 1974

TR 77161

Fig 20

Mean radiance
(ωm^{-2} ster^{-1} μm^{-1})

3

2

1

-80   -60   -40   -20   0   +20   +40   +60   +80
(South)   Latitude   (North)

Standard deviation
(ωm^{-2} ster^{-1} μm^{-1})

0.4

0.3

0.2

0.1

-80   -60   -40   -20   0   +20   +40   +60   +80
(South)   Latitude   (North)
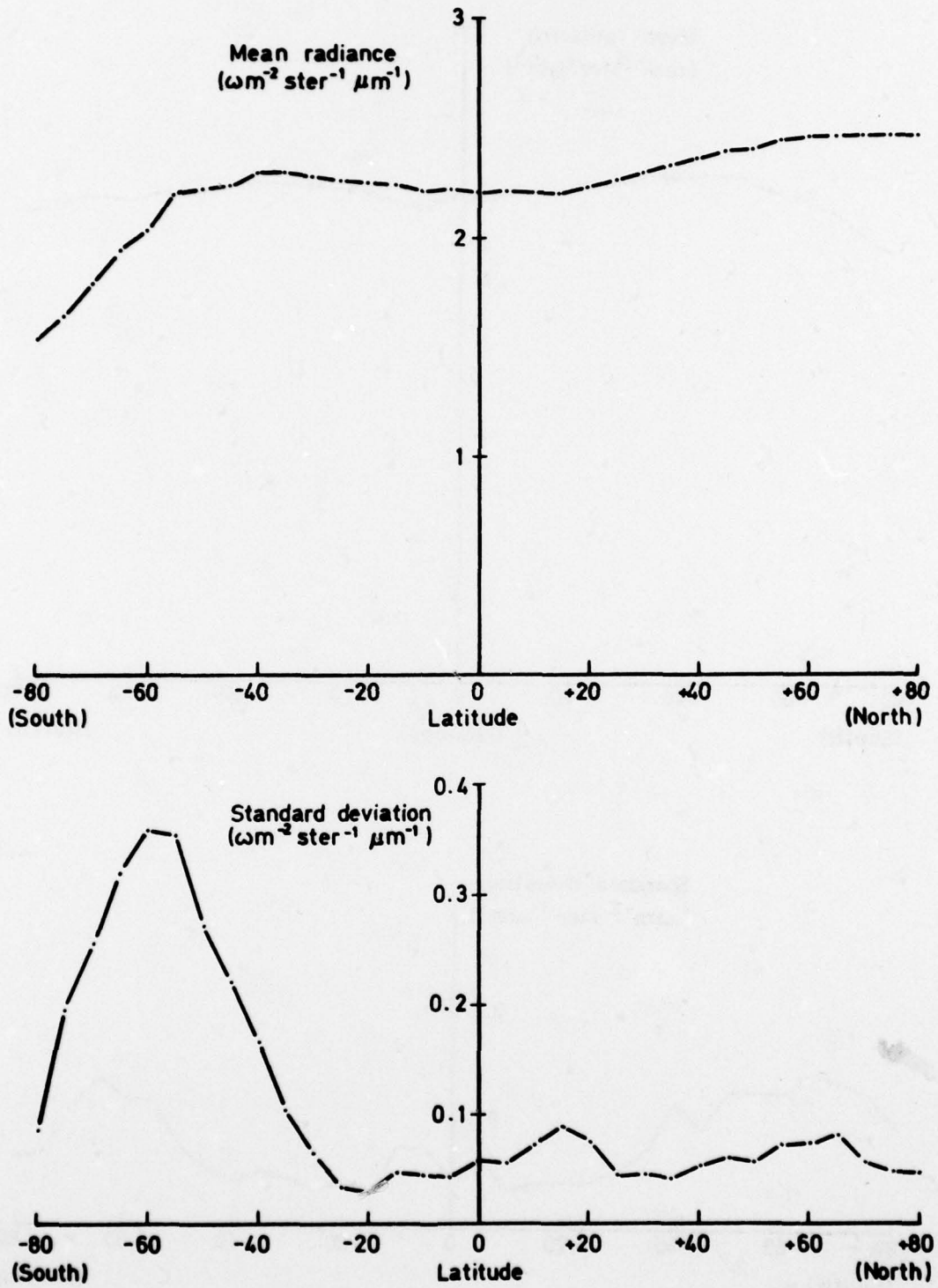
Fig 20   Earth radiance — 9-12 September 1974

TR 77161
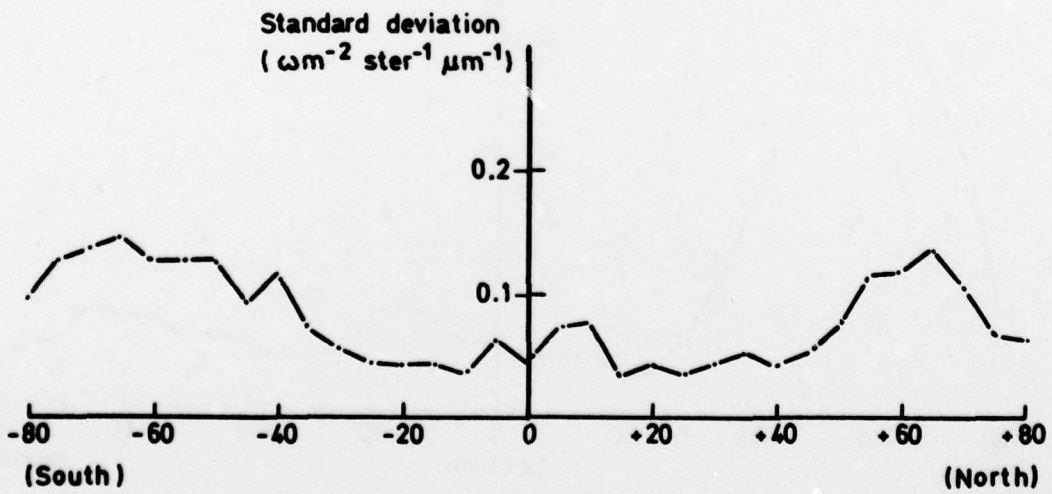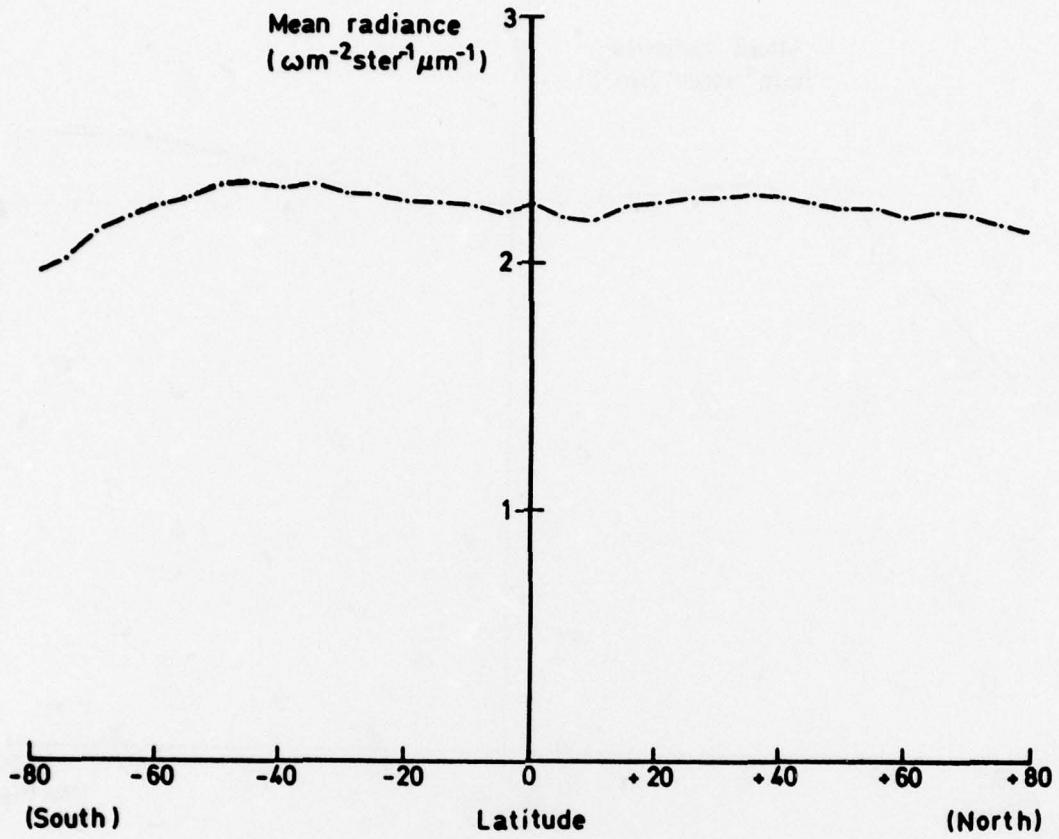
Fig 21

Fig 21   Earth radiance — 6-10 October 1974
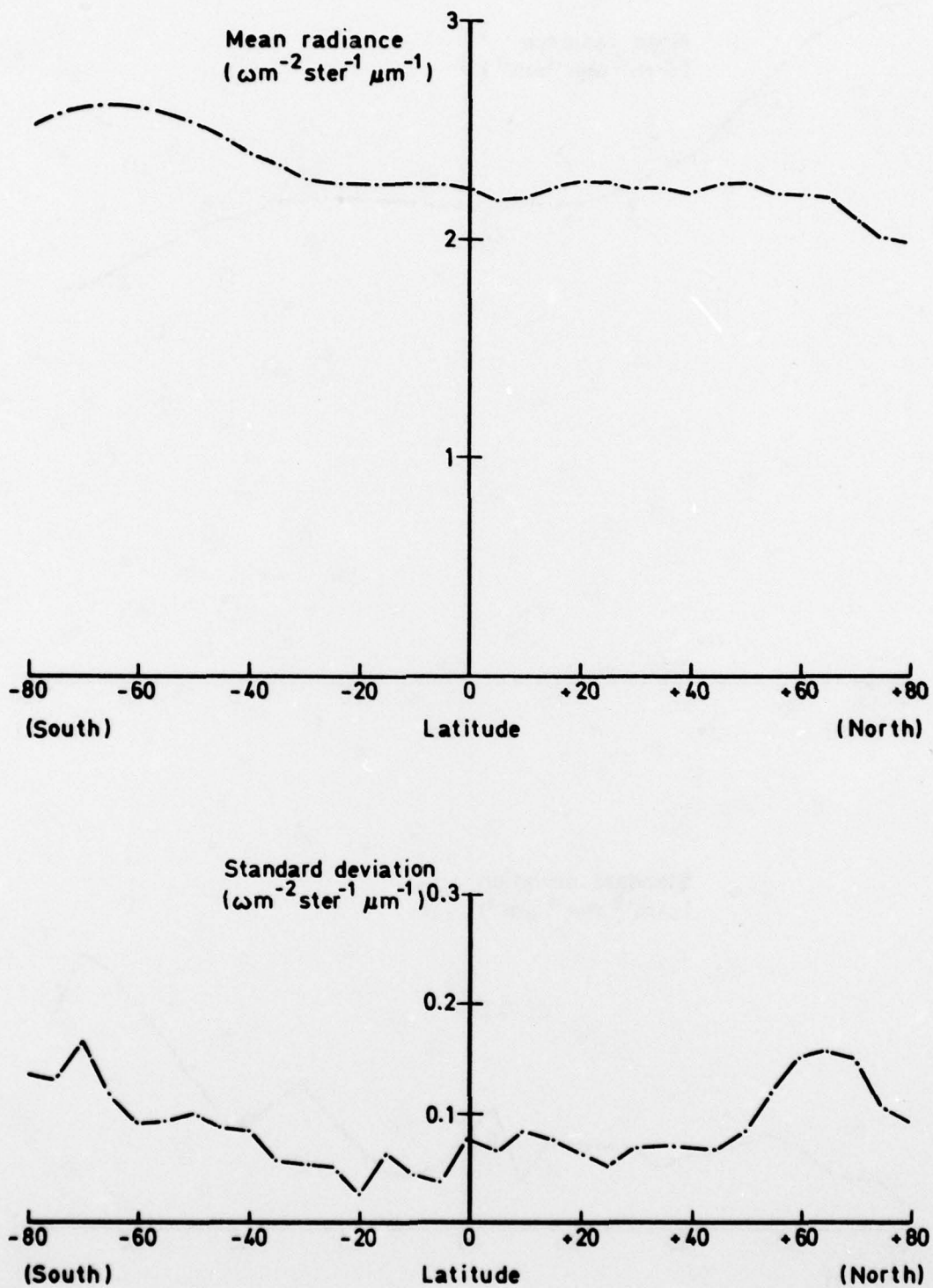
Fig 22

Fig 22   Earth radiance – 30 October-1 November 1974
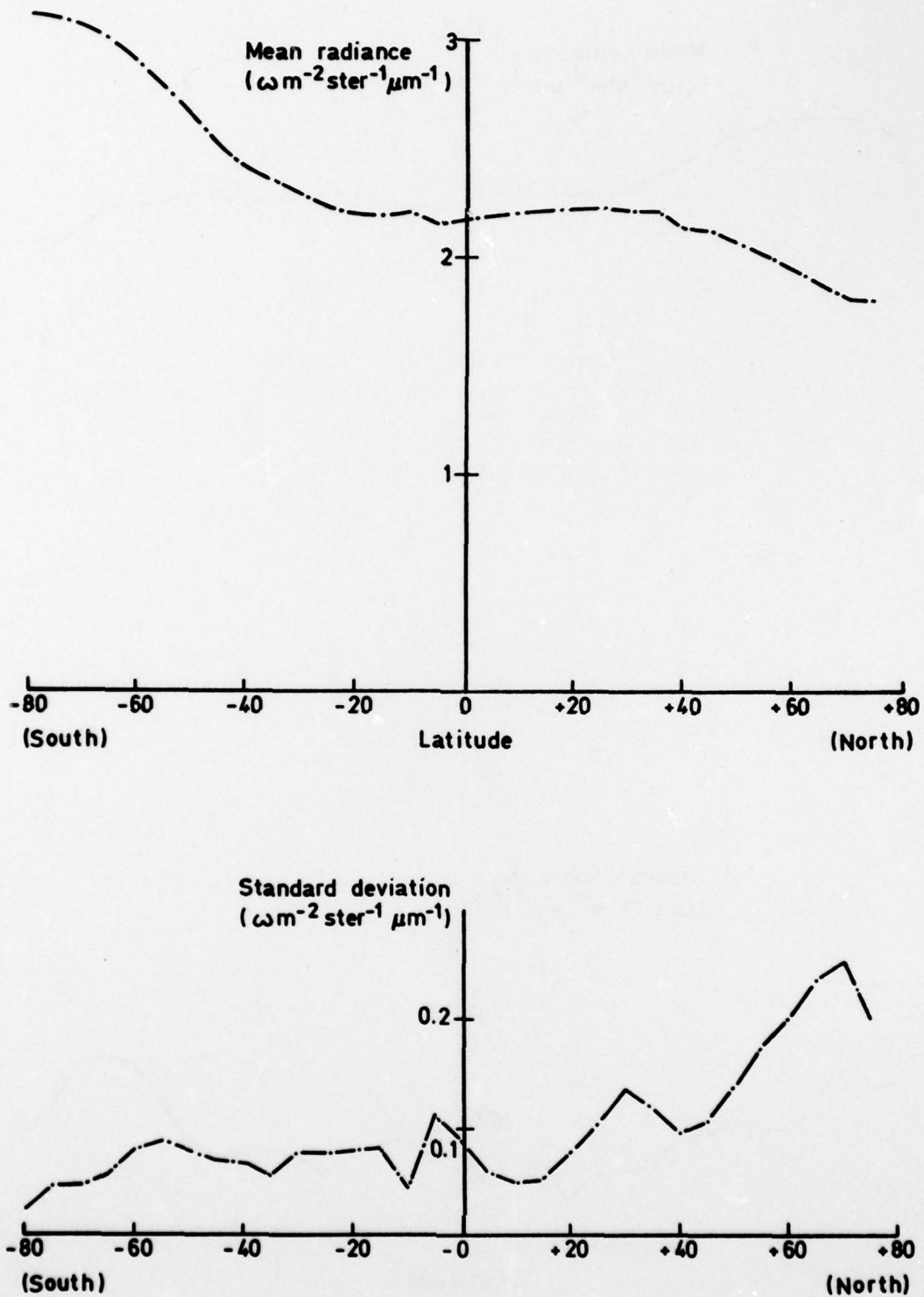
Fig 23   Earth radiance — 26-29 November 1974
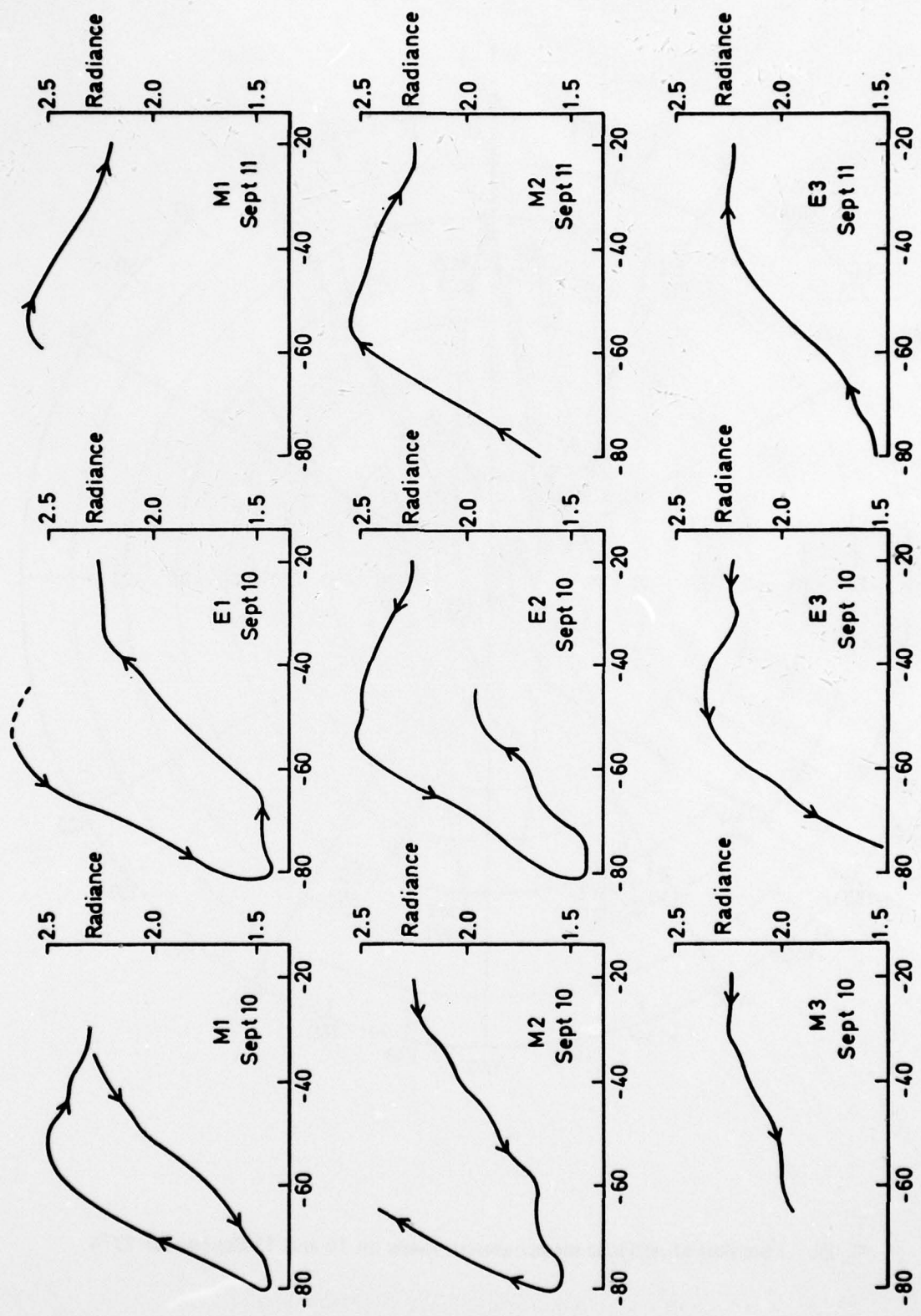
Fig 24

Fig 24 Radiance (ω m^{-2} ster^{-1} μm^{-1}) data from individual orbits — 10 and 11 September 1974
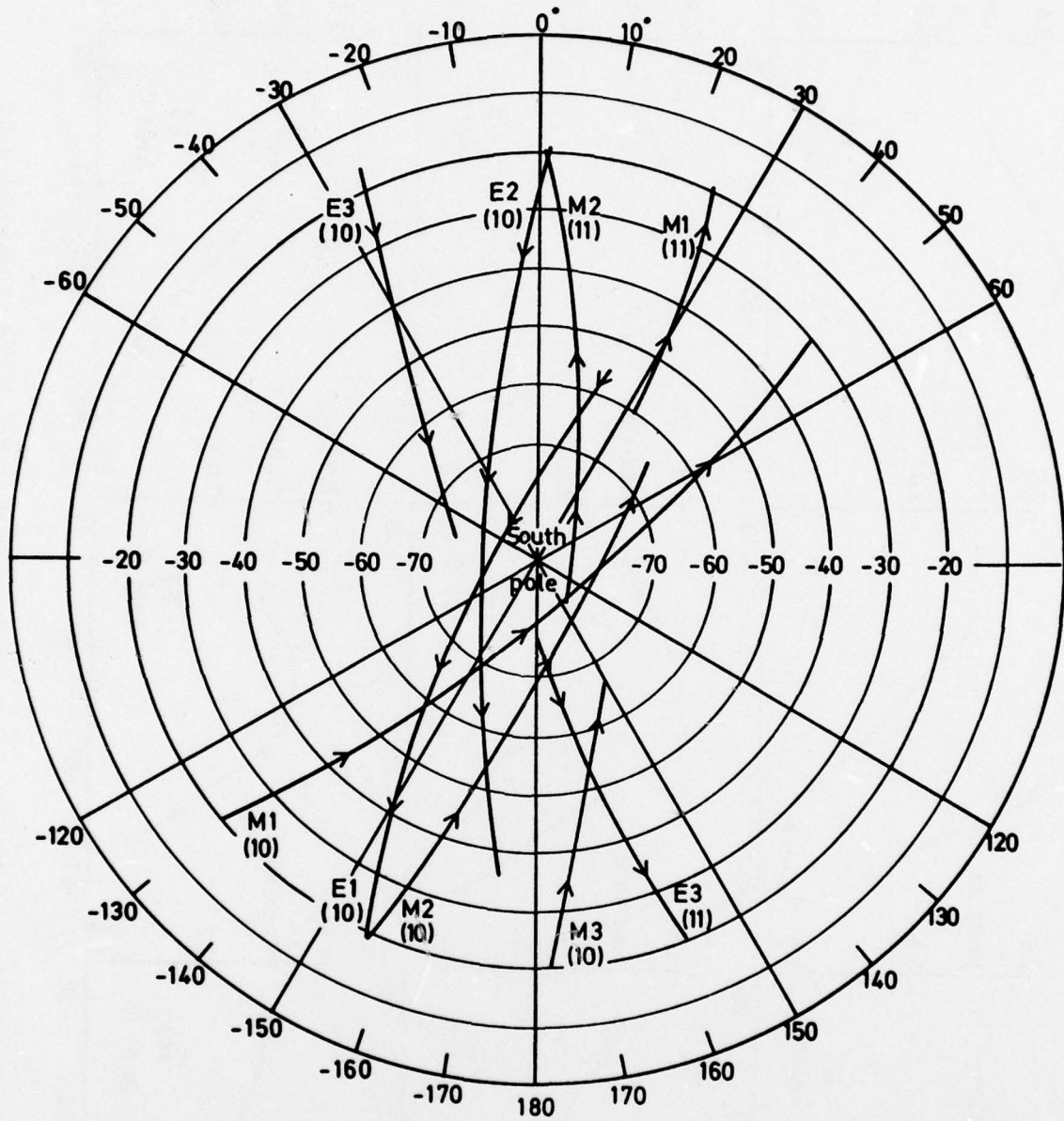
Fig 25

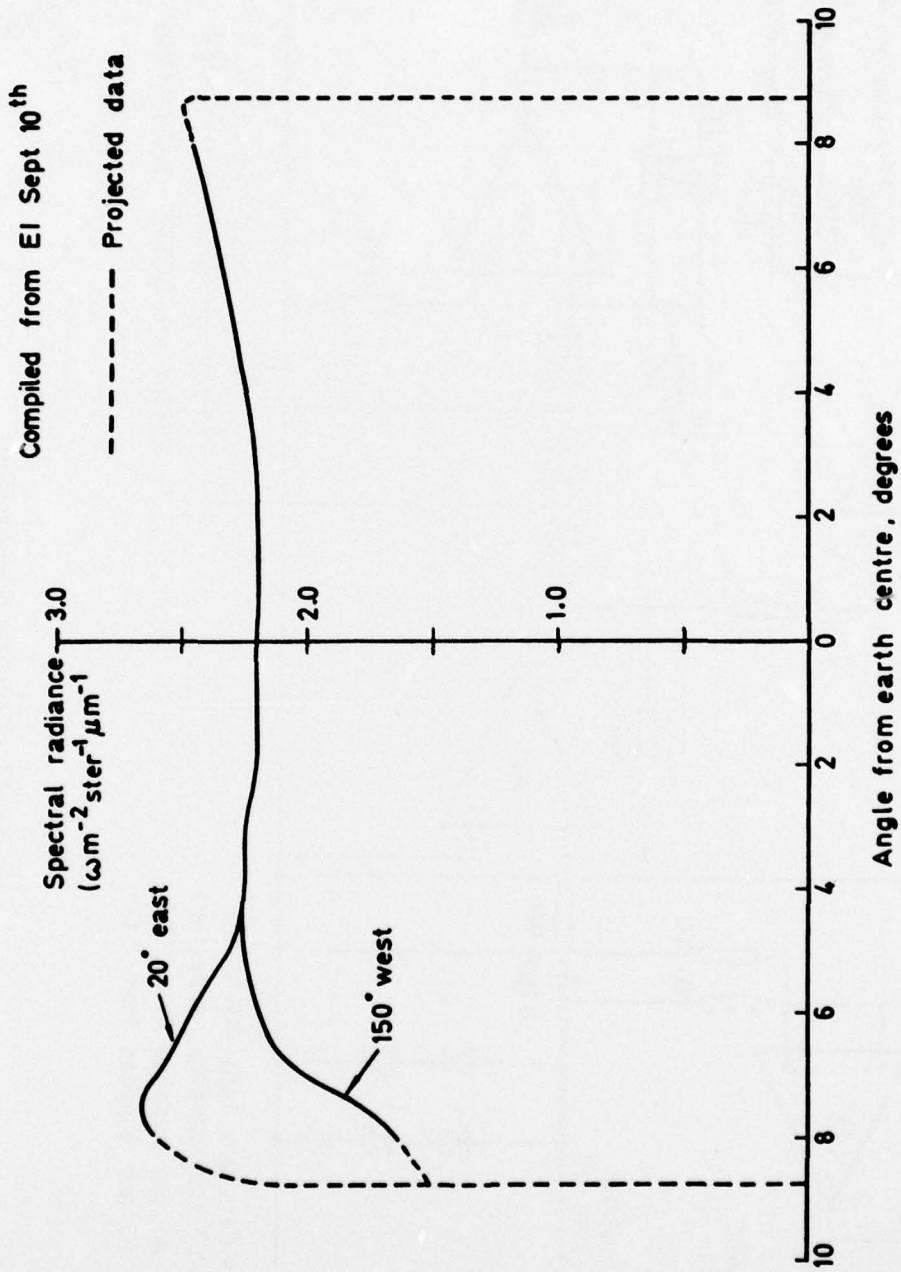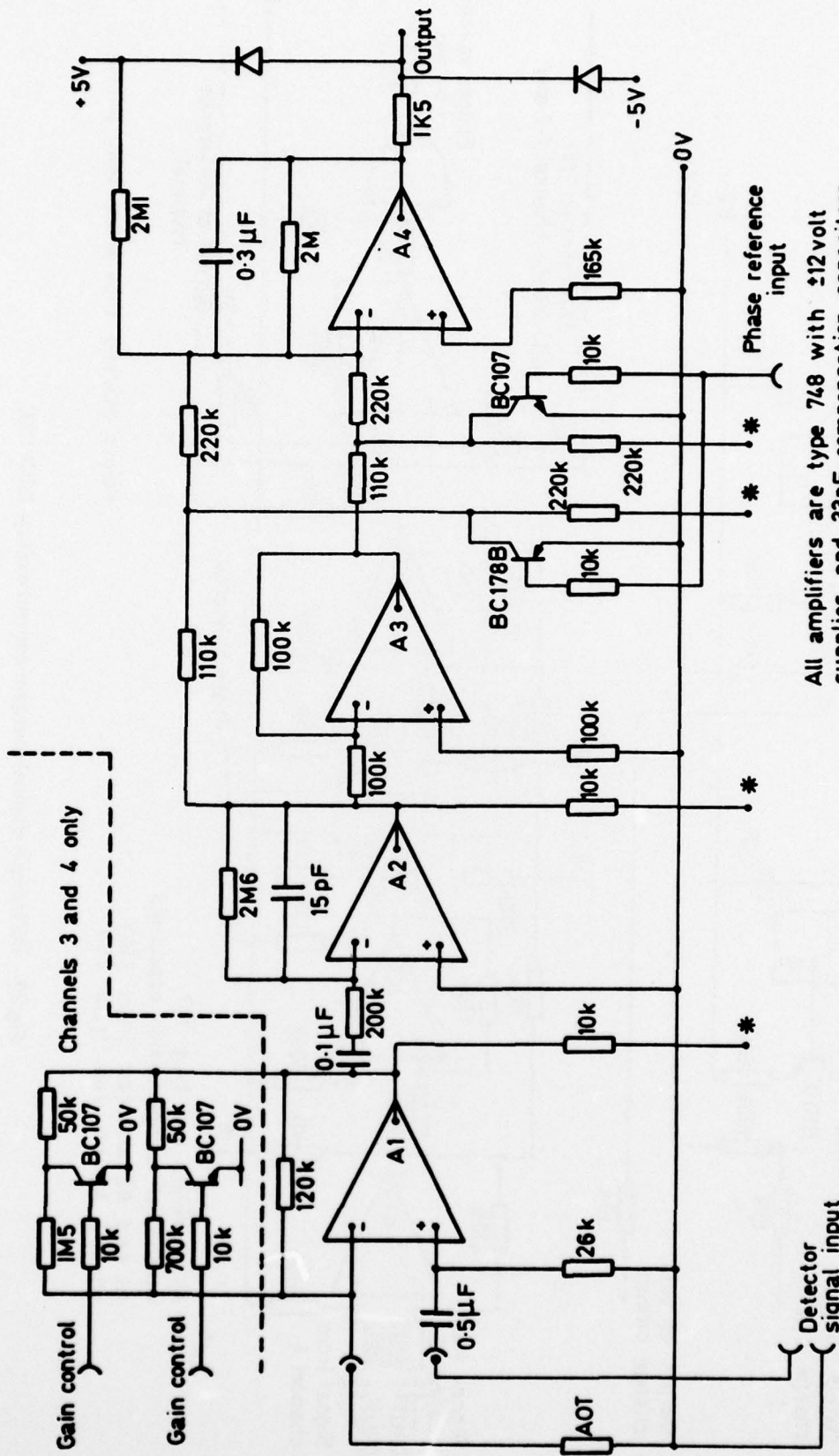**Fig 25   Location of radiance measurements made on 10 and 11 September 1974**

Fig 26

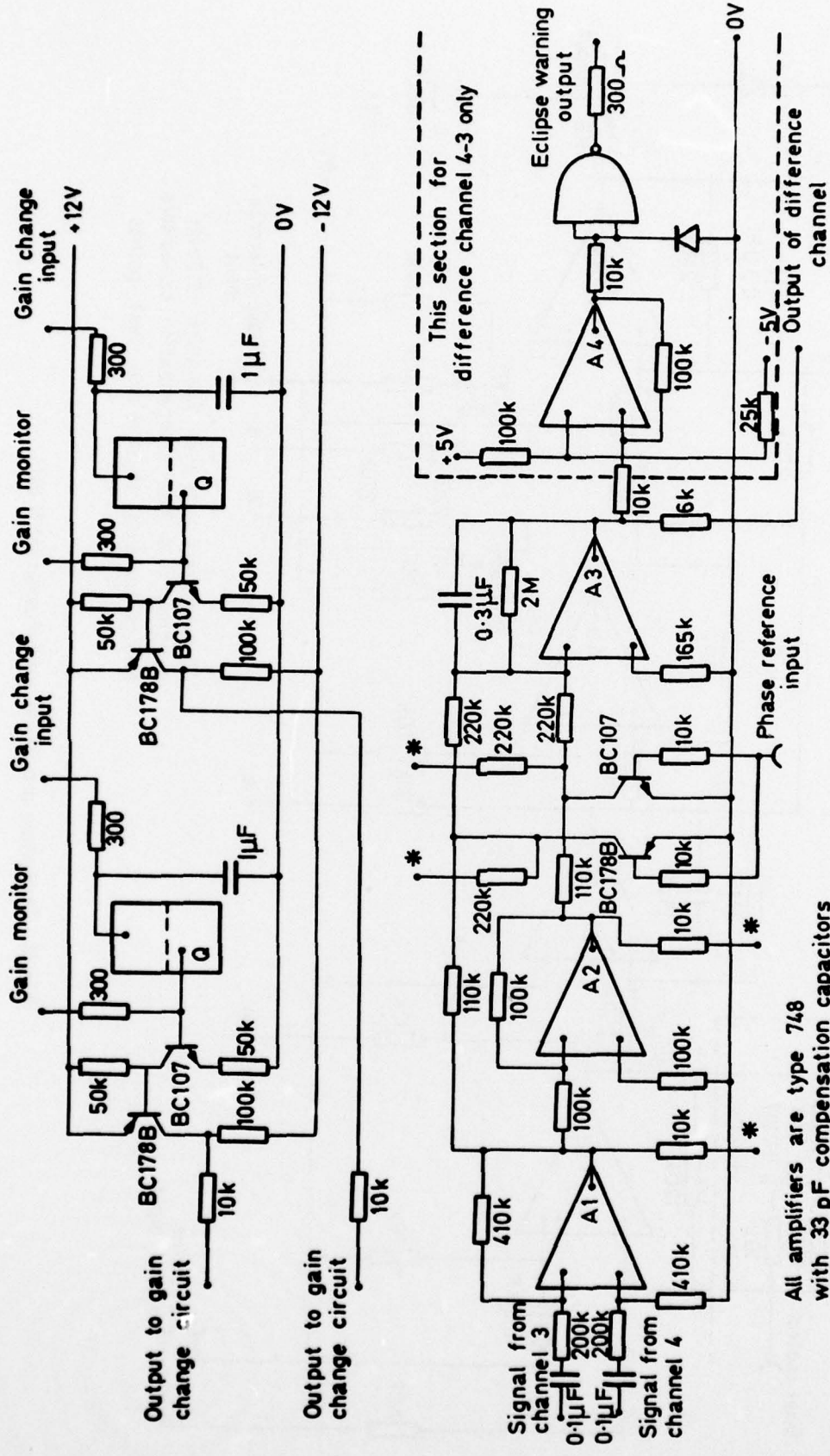Fig 26 Radiance patterns at 20° east and 150° west from geosynchronous orbit

Fig 27

Fig 27   Modulator drive circuitry

TR 77161

Fig 28

Fig 28   Processing circuitry for one channel (MCI IS1)

All amplifiers are type 748 with ±12 volt
supplies and 33pF compensation capacitors
Points marked thus * are test points

TR 77161

Fig 29

Fig 29   Difference channel and gain control circuits (MCI IS3)

REPORT DOCUMENTATION PAGE

Overall security classification of this page

UNCLASSIFIED

As far as possible this page should contain only unclassified information. If it is necessary to enter classified information, the box above must be marked to indicate the classification, e.g. Restricted, Confidential or Secret.

1. DRIC Reference (to be added by DRIC)	2. Originator's Reference RAE TR 77161	3. Agency Reference N/A	4. Report Security Classification/Marking UNCLASSIFIED

5. DRIC Code for Originator 850100	6. Originator (Corporate Author) Name and Location Royal Aircraft Establishment, Farnborough, Hants, UK

5a. Sponsoring Agency's Code N/A	6a. Sponsoring Agency (Contract Authority) Name and Location N/A

7. Title The Miranda (X4) infra-red experiment: design, performance and earth radiance measurements

7a. (For Translations) Title in Foreign Language

7b. (For Conference Papers) Title, Place and Date of Conference

8. Author 1. Surname, Initials Barnes, M.B.	9a. Author 2 Craig, S.	9b. Authors 3, 4 .... Haskell, A.	10. Date November 1977	Pages 45	Refs. 3

11. Contract Number N/A	12. Period N/A	13. Project X4	14. Other Reference Nos. Space 538

15. Distribution statement
(a) Controlled by – MOD(PE) D Space

(b) Special limitations (if any) –

16. Descriptors (Keywords) (Descriptors marked * are selected from TEST)

Miranda X4. Infra-red pyro-electric detector. Earth sensor. Earth radiance.

17. Abstract

A description of the infra-red experiment carried on the UK Miranda (X4) satellite is given. The performance of the four pyro-electric detectors used in the experiment is described and details of the technique used for measuring the radiance of the earth in the band 14-16 µm are presented. Finally the measured radiance of the earth is shown for periods at monthly intervals from March to November 1974 and the implications of these results for the design of infra-red earth sensors are discussed.

Micrometers

RAE Form A143